U.S. DEPARTMENT OF COMMERCE
National Technical Information Service

PB-260 050

CORONA TREATMENT OF WASTE WATER

General Electric Company
Schenectady, New York

14 May 1965

257175

PB 260 050

ADVANCED TECHNOLOGY LABORATORIES

CORONA TREATMENT OF WASTE WATER

By

W. R. Browne and E. E. Stone
Advanced Technology Laboratories
General Electric Company
Schenectady, New York

14 May 1965

GENERAL ELECTRIC

REPRODUCED BY
NATIONAL TECHNICAL
INFORMATION SERVICE
U. S. DEPARTMENT OF COMMERCE
SPRINGFIELD, VA. 22161

BIBLIOGRAPHIC DATA SHEET	1. Report No.	2.	3. Recipient's Accession No. PB-260 050
4. Title and Subtitle Corona Treatment of Waste Water			5. Report Date 14 May 65 6.
7. Author(s) W. R. Browne and E. E. Stone			8. Performing Organization Rept. No.
9. Performing Organization Name and Address General Electric Co., Schenectady, N. Y. Advanced Technology Labs.			10. Project/Task/Work Unit No. 11. Contract/Grant No. PH-86-64-142
12. Sponsoring Organization Name and Address Advanced Waste Treatment Program, Cincinnati, Ohio.			13. Type of Report & Period Covered 14.

15. Supplementary Notes

16. Abstracts The performance of two corona reactors, falling film type and rotating disk type, were evaluated for their efficiency in oxidizing a ferrous sulfate solution in the presence of moist air. The falling film type was found to be superior and additional studies were conducted to characterize those process variables which affected reactor performance. From the data a linear least squares regression equation was derived, giving an approximation of the underlying relationships. The falling film type was also evaluated for its ability to oxidize aqueous solutions of benzoic acid, alkyl benzene sulfonate, filtered secondary effluents, and effluents from a carbon adsorption column. The easily oxidized ferrous ion reacted with corona activated species which did not strongly attack the organic materials.

17. Key Words and Document Analysis. 17a. Descriptors

17b. Identifiers/Open-Ended Terms
*Waste water
*Waste treatment research
*Electric reactors
Reactors
Radiation sources

17c. COSATI Field/Group 13B

18. Availability Statement	19. Security Class (This Report) UNCLASSIFIED	21. No. of Pages 76
	20. Security Class (This Page UNCLASSIFIED	22. Price

FORM NTIS-35 (REV. 10-73) ENDORSED BY ANSI AND UNESCO. THIS FORM MAY BE REPRODUCED USCOMM-DC 8265-P74

CORONA TREATMENT OF WASTE WATER

By

W. R. Browne and E. E. Stone
Advanced Technology Laboratories
General Electric Company
Schenectady, New York

For

The Advanced Waste Treatment Research Program
Basic and Applied Sciences Branch
Robert A. Taft Sanitary Engineering Center

A report submitted in fulfillment of a contract between
The Public Health Service and the General Electric Company
(PH 86-64-142)

ABSTRACT

The performance of two corona reactors (1) falling film type and (2) rotating disk type were evaluated for their efficiency in oxidizing a ferrous sulfate solution in the presence of moist air. (1) was found to be superior and additional studies were conducted to characterize those process variables which affected reactor performance. From the data a linear least squares regression equation was derived, giving an approximation of the underlying relationships. (1) was also evaluated for its ability to oxidize aqueous solutions of benzoic acid, alkyl benzene sulfonate, filtered secondary effluents, and effluents from a carbon adsorption column; corona power averaged 58 KWH/1000 gal./10 COD for these solutions. Evidence obtained indicated that the easily oxidized ferrous ion reacted with corona activated species which did not strongly attack the organic materials.

TABLE OF CONTENTS

	Page
INTRODUCTION	1
SCOPE OF WORK	2
CORONA EQUIPMENT AND MEASUREMENT OF CORONA POWER	2
(I) EVALUATION OF CORONA REACTORS	6
Falling Film Reactor	6
Rotating Disk Reactor	10
Conclusion	13
(II) DETERMINATION OF PERFORMANCE CHARACTERISTICS CHARACTERISTICS FOR FALLING FILM SWIRL REACTOR	15
Test Objective	15
Reactor Design	19
Operating Procedure	23
Variability of the Process	23
Results of Test	25
Oxygen and Electrode Gap Tests	41
Miscellaneous Tests	41
(III) ORGANIC OXIDATION	43
Public Health Service Tests	43
(IV) ECONOMIC CONSIDERATIONS	45
Motor-Generator Set	46
High-Voltage Transformer	47
Tuning or Power Factor Correction Circuit	47
Control and Instrumentation	47
Corona Reactor	48
Costs	48
SUMMARY OF THE FOUR PROJECT PHASES	51
ACKNOWLEDGEMENTS	53
REFERENCES	54
APPENDIX A	
APPENDIX B	
APPENDIX C	

INTRODUCTION

Corona is a soft electrical discharge which is prevented from becoming an arc by either geometry or the presence of a solid dielectric barrier. It is a relatively cool, high-voltage, low-current capacitive discharge, unlike an arc which is characterized by high temperature, low voltage, and high current. The reactions associated with an arc result from thermal activation. As in radiation chemistry, active species in corona are produced by electron bombardment. The electrons leave the electrodes and enter into secondary reactions with the gaseous molecules in the discharge space. At atmospheric pressure the electron energies have a distribution from near zero electron volts to values slightly greater than the ionization potential of the gas in which the discharge occurs[3,7]. Either directly or indirectly, collision of these electrons with the gas molecules may produce a great variety of species such as excited atoms, ions, and free radicals after the manner of radiolysis.

The most frequent reaction is thought to be that of an orbital electron being lifted to a higher energy level forming an excited molecule, which then decays into two free radicals (in the case of a diatomic molecule). The free radicals then recombine in the usual random way.

When moist air or oxygen is passed through a corona zone the species H, OH, OH^-, and HO_2 are generated. Their oxidizing activity during recombination reactions is well known. One of the best understood systems (from the field of radiation chemistry) is the ferrous to ferric conversion initiated by radiation. Allen's discussion[1] has recently been extended by Hart[8] to introduce the hydrated electron concept. Typical reaction mechanisms are:

$$H + O_2 = HO_2$$

$$HO_2 + Fe^{+2} = HO_2^- + Fe^{+3}$$

$$HO_2 + Fe^{+2} + H^+ = H_2O_2 + Fe^{+3}$$

$$H_2O_2 + Fe^{+2} = OH + OH^- + Fe^{+3}$$

$$OH + Fe^{+2} = OH^{-} + Fe^{+3}$$

$$H + H^{+} + Fe^{+2} = H_2 + Fe^{+3}$$

Similar reactions would be expected to occur in the presence of organic materials particularly if the HO_2 and H_2O_2 molecules could be brought within the reaction sphere of the organic material. Extension of this idea led to the concept of subjecting waste and polluted water to the action of corona generated species. Thus, the purpose of this study was to evaluate the feasibility of corona treatment for upgrading the quality of the water.

SCOPE OF WORK

The initial program involved (I) the study of two different corona reactors to determine which reactor offered the greater promise for scale-up studies of waste water treatment, (II) the determination and characterization of those process variables which affect reactor oxidation performance, (III) the preliminary study of the corona reactor oxidation efficiency on various organic solutions including secondary and carbon-treated waste water effluents, and (IV) the preliminary economic analysis of treating waste water to determine the economic feasibility of the corona process. The ferrous-ferric oxidation system was used in the evaluation of the reactor type (I) and process variables (II) with the mg. of ferric produced per watt-hour as the decisive criterium.

CORONA EQUIPMENT AND MEASUREMENT OF CORONA POWER

The corona generating equipment consists of five major components: a high voltage interlocked cage for housing the test equipment; a power supply for the generation of the required high voltage; a device for converting low-frequency power to high-frequency power; a corona reaction cell; and instrumentation to permit measurement and control of the power supply, corona, and other critical electrical parameters. A motor-alternator generates the required voltage by varying the field winding of the 10,000 cycle alternator

which feeds the primary of a high voltage transformer (Figure 1). A choke and a capacitor bank are used in parallel with the corona reactor and present a "tuned circuit" to the transformer for efficient power utilization. The crest voltmeter indicates peak voltage rather than rms values.

The oscilloscope displays the relationship between the voltage applied to the reactor electrodes and the charge flow in the circuit. Before corona occurs, the oscilloscope figure is a slant line. As corona forms, the slant line opens to a parallelogram figure; the area of which, after proper calibration, is directly related to the power dissipated in the reactor.

The parallelogram technique for measuring corona power is a modification of an approach developed by Manley[11]. It dates back to early high voltage and corona oscillogram measurements which H. J. Ryan[14], and F. W. Peek, Jr.[13] reported about the turn of the last century.

A bridge circuit, with separate "voltage" and "charge" branches utilizing capacitance voltage dividers feeds proportional signals to the X-Y axes of the oscilloscope. The X-Y product, then, is a measure of the energy per cycle dissipated in the cell. The multiplication of the X-Y product by the frequency is the total power.

This approach to corona power measurement, however, is an experimental laboratory technique and should not be construed as having any specific production line tolerances and accuracy. The many possible sources of error are:

1. The measurement of the high voltage applied to the cell. (The voltage axis calibration of the oscilloscope is affected by the high voltage capacitance divider and the full scale tolerance of the high voltage voltmeter.)

2. The determination of the charge flowing through the corona cell. (The measurement is affected by the tolerance of the capacitors in the "charge" branch of the bridge circuit and the charge axis calibration of the oscilloscope.)

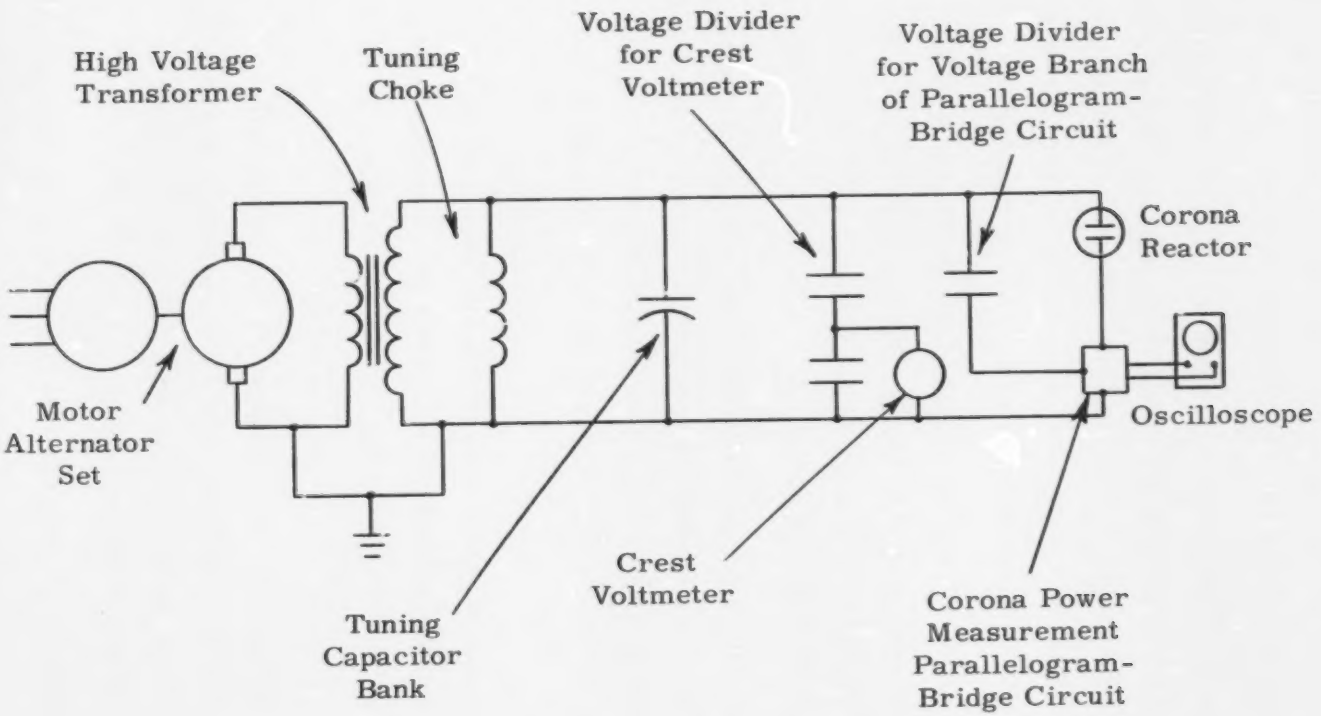

Figure 1 Basic Power and Instrumentation Circuit

3. The accuracy of power supply frequency determination.
   (The frequency is a factor in the final calibration figure.)

4. The determination of parallelogram area and shape.
   (This is the greatest possible source of error. The shape and clarity of the parallelogram figure is affected by the steadiness of cell corona, and by the corona cell characteristics.)

The parallelogram area may be determined in several ways:

a. Photographing the parallelogram on the oscilloscope with a Polaroid camera and measuring the area with a planimeter, noting any scale factors involved.

b. Tracing the parallelogram area with wax pencil on a transparent film material and measuring the figure.
   (This method provides a means of holding the wattage constant and noting any changes in the shape of the parallelogram.)

c. Measuring the parallelogram directly with a flexible, transparent, centimeter scale.

Best accuracy is obtained with the largest parallelogram figure that can be completely contained on the oscilloscope.

Comparison of area estimates made by method c, above, on different oscilloscope ranges showed that it is possible to get agreement on area estimates within ten percent. If the tolerances on all aspects of corona power measurement were to add up in the same direction, the error in measurement might be as great as twenty percent. A comparison of the parallelogram-oscilloscope technique with other methods of measuring corona power showed close agreement, and indicated that the probable error was more likely within fifteen percent.

A calorimetric check of corona power showed the parallelogram power measurement to be 17 percent lower than the calorimetric power.

A comparison of high voltage transformer primary power measurements made with a high frequency wattmeter, and secondary power measurements made with the parallelogram-oscilloscope technique (including provision for transformer losses) gave results agreeing within fifteen percent, with the parallelogram measurement being on the low side. A comparison of parallelogram power measurement method with power measurements made by a GE-ATL developed corona wattmeter showed agreement within 5 to 15 percent, with the parallelogram measurement once again on the low side. This pattern of low-side parallelogram power measurements probably indicated a tendency in this laboratory to be conservative in the measurement of parallelogram area.

(I) EVALUATION OF CORONA REACTORS

Two types of corona reactors, the falling film reactor and the rotating disk reactor, were evaluated by their performance in oxidizing ferrous ion in a dilute sulfuric acid solution. A feed with a concentration of 80 mg Fe^{+2}/l, the same as recommended by Allen[1] for determining gamma-ray dosages, was prepared following the procedure given in Appendix A. After exposure to the corona, the extent of conversion of the ferrous ion to ferric ion was determined from spectrophotometric measurements as described in Appendix B. The basis for comparison of the reactors was the amount of Fe^{+3} produced per watt-hour.

Falling Film Reactor

This reactor, made of quartz, (Figure 2) consisted of two vertically mounted concentric cylinders fitted with standard taper gas and liquid attachments. The corona generating portion of the reactor is the long straight section made up of the outer quartz tube, gas gap, and inner quartz tube. In operation, feed solution flowed in the gas gap against the outer wall; it was forced through the inlet jet under sufficient pressure to cause the liquid to encircle the reactor wall resulting in a liquid film falling through the corona zone. The central cylinder served as the high potential electrode and was closed off at the lower end. Cooling water, which flowed through this electrode, was isolated electrically by an insulated loop of suitable

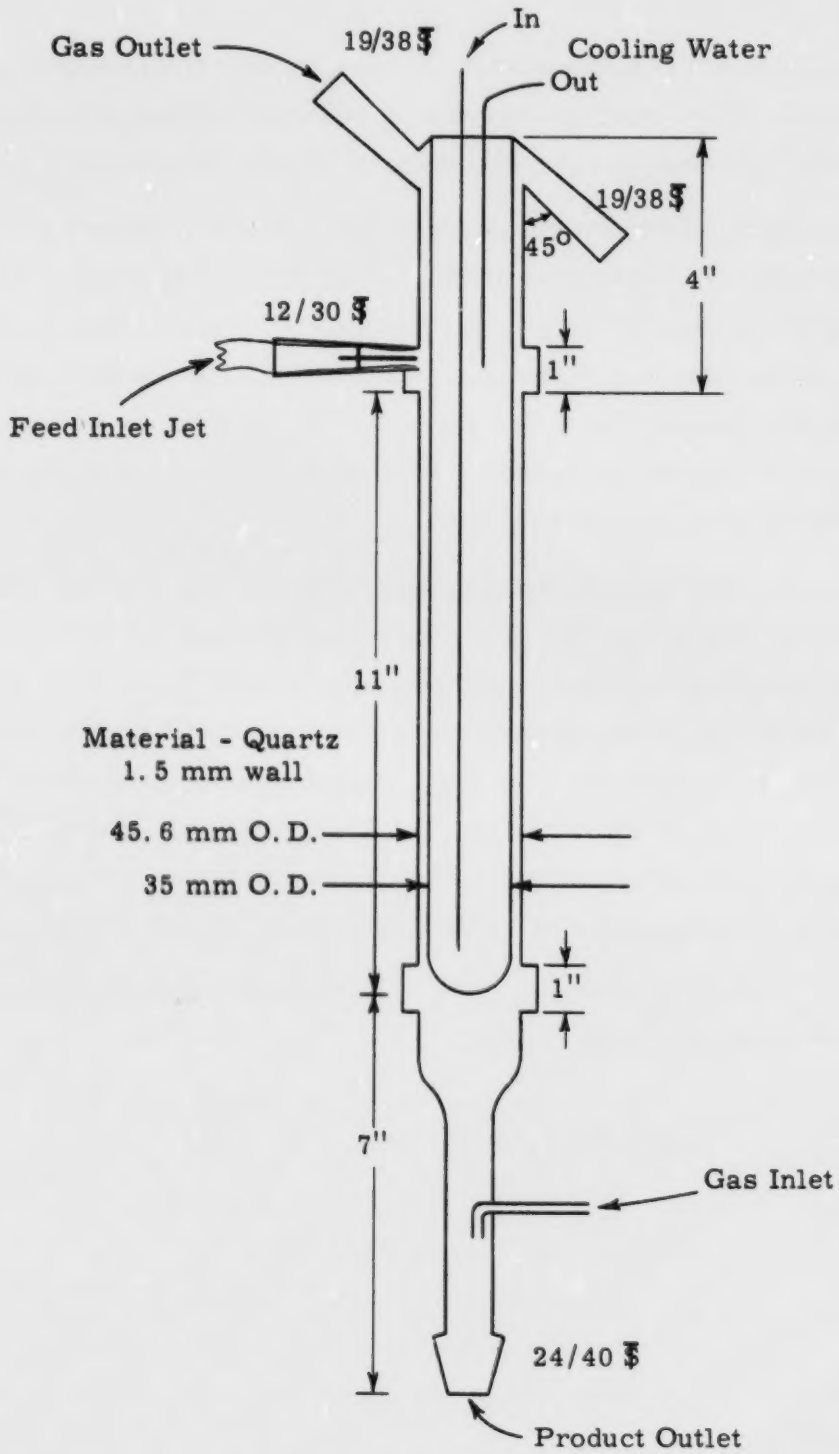

Figure 2. Falling Film Reactor

length to provide a high resistance path to ground. A conductive coating applied to the outside of the reactor over the eleven-inch section served to define the corona zone and complete the electrical circuit to the ground.

The reactor electrode spacing was 7.6 mm. It contained a volume of 128 ml between the electrodes of the corona zone. The logarithmic mean cross-sectional area of the gap was 339 cm^2. Figure 3 illustrates the flow paths of the gas and liquid streams. The operating procedure consisted of 1) setting the gas and liquid flow rates, 2) bringing up the voltage to start corona and to achieve the desired power level, and 3) collecting samples of the corona treated ferrous solution.

Fourteen runs were made at various power levels and flow rates using a feed solution with a ferrous sulfate concentration of about 80 mg/l. Exact test conditions and results are given in Appendix C, Table I. The first series of three tests were inconclusive because of poor liquid distribution in the reaction zone. Installation of a larger liquid feed jet appeared to correct the flow problem, and in the next series of three runs, all of the Fe^{+2} was converted under the test conditions. The other runs gave yield values which appeared to be independent of liquid flow rate and power density.

Yield values, or the amount of Fe^{+3} produced for a given quantity of power, were calculated as follows:

$$\text{Yield} = \frac{FC}{P}$$

where,

Yield = mg Fe^{+3}/watt-hour.

F = flow rate, l/hr.

C = Fe^{+3} concentration, mg/l

P = power, watts

The average yield value was 7.91 with a standard deviation of 2.41.

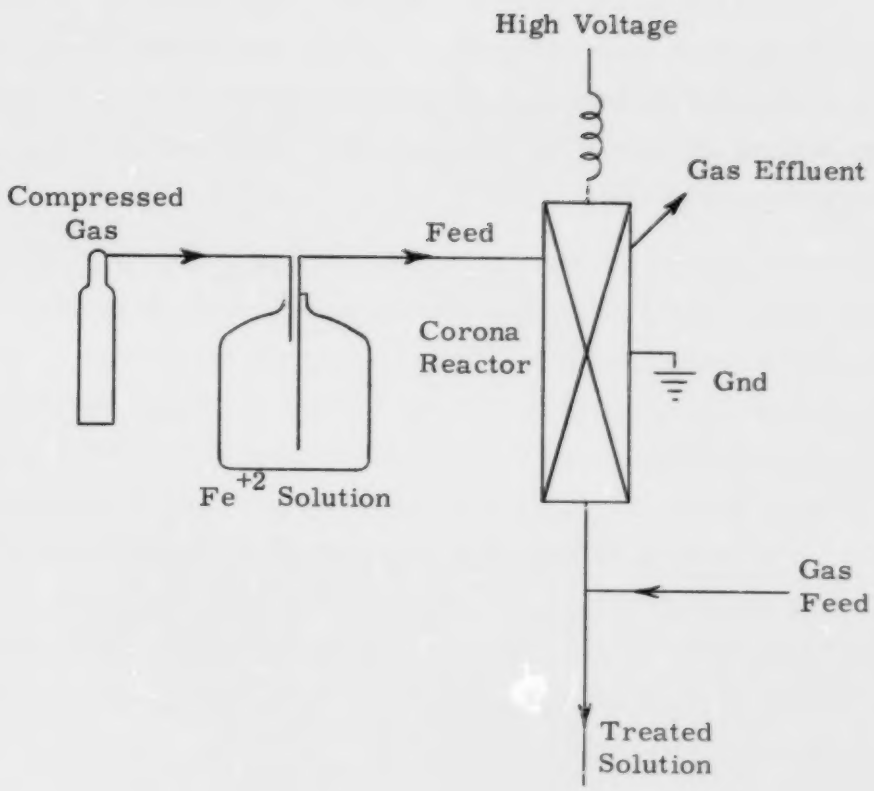

Figure 3. Falling Film Reactor Flow Diagram.

Rotating Disk Reactor

This reactor (Figure 4) consisted of a vertical stainless steel disk 11.1-cm dia.) which rotated in a 13.3 cm diameter chamber formed by two parallel quartz plates and the insulating shell of Textolite. The centrally located disk was spaced 0.60 cm from each of the quartz plates and corona formed on both sides of it in a zone defined by a 14 cm^2 annular segment of conductive coating applied to the outside of each of the quartz plates. High potential was applied to the plates; grounded potential to the disk.

Suitable liquid and gas attachments were provided around the rim of the shell. In operation, feed solution flowed continuously into the reactor filling the lower half of the chamber (56 cm^3) and leaving via an overflow. Gas, admitted beneath the liquid surface, bubbled through the liquid and was vented near the top of the chamber. As the disk rotated through the pool of liquid it picked up a film of liquid and transported it through the corona zone at a controlled speed. The factors influencing the amount of material transported (a function of the liquid properties and the disk size and speed) have been discussed by Staub and Brisee[16]. Figure 5 shows this relationship over the speed range of 1 to 30 rev/min which corresponds approximately to 2.5 to 600 ml/min of transported liquid.

A series of five runs was made using a feed concentration and power density that would permit a comparison with the falling film data. The procedure was to set the liquid and gas flows, to adjust the disk speed, then to bring the corona power up to the test value. Periodic samples were taken to follow the conversion of Fe^{+2} to Fe^{+3}. The liquid level was set to submerge one-half of the disk and the liquid flow rate was maintained as high as possible to hold this liquid level.

Table II of Appendix C contains the data for these runs. The first run was conducted to test the operating procedure and stability of flow rates. The second and third runs were made to show the effect of changing disk speed. For both of these runs rather poor conversions were obtained. As evidenced from the analytical data, equilibrium operating conditions were not attained.

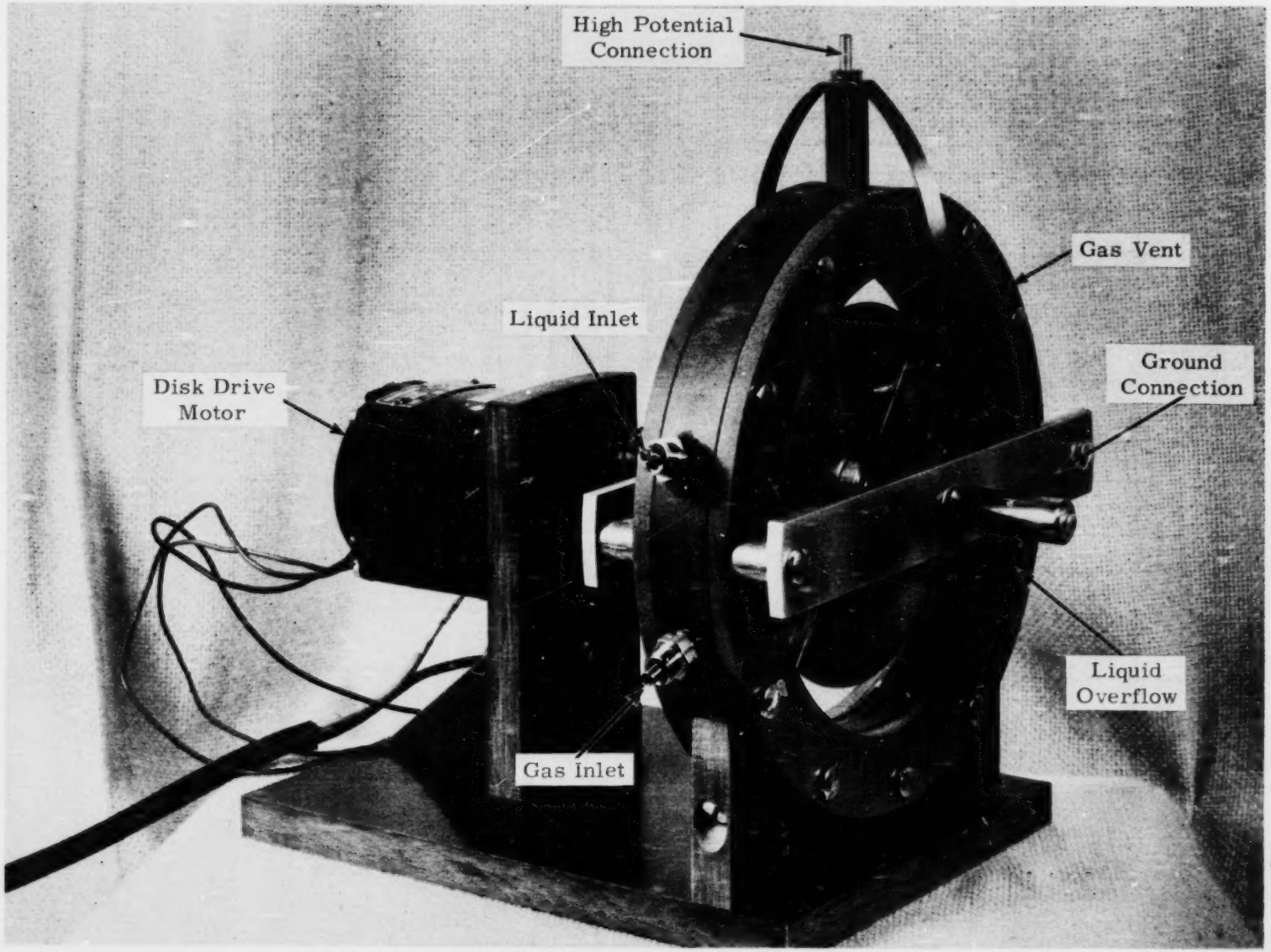

Figure 4. Single-Plate, Rotating Disk Reactor

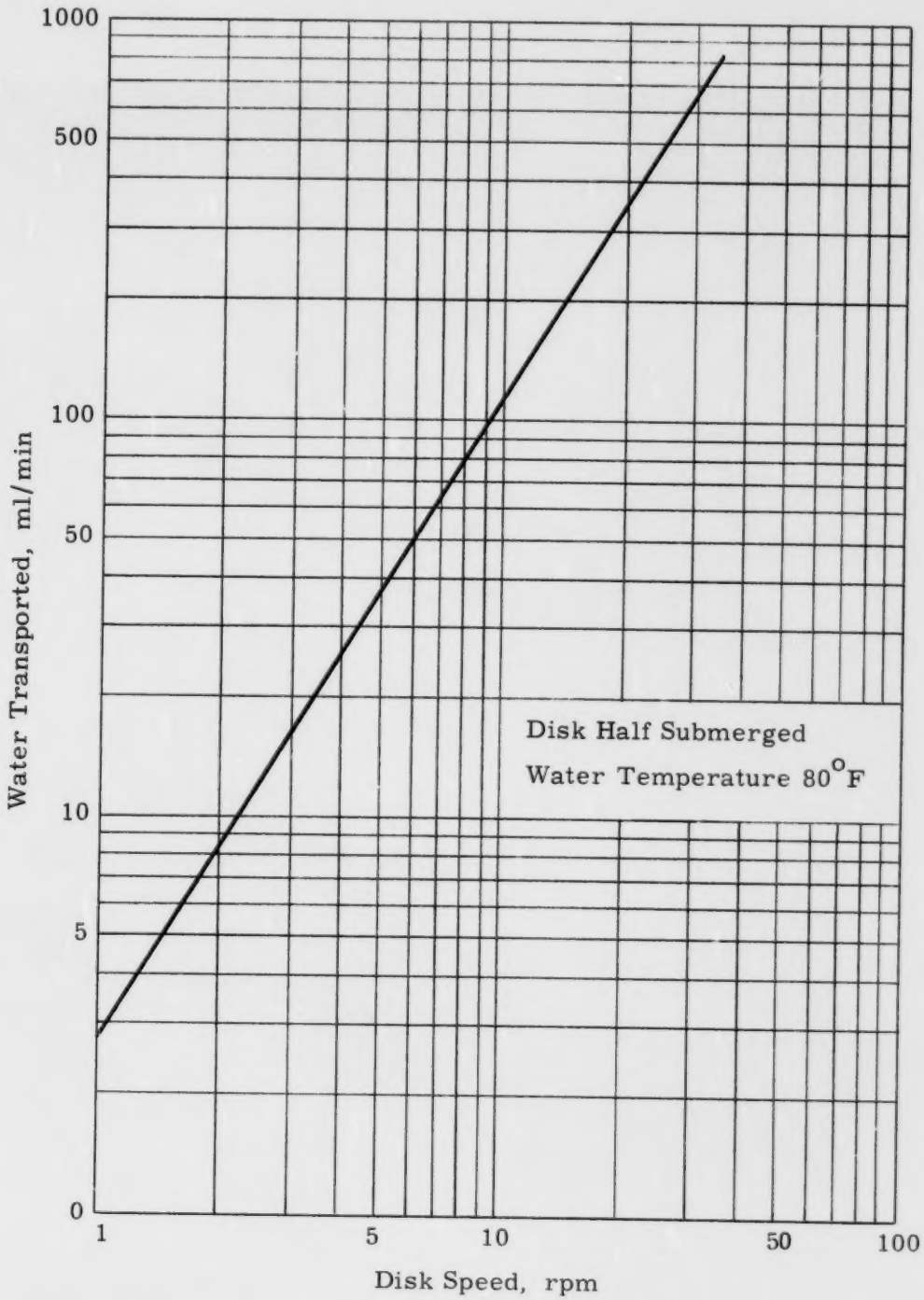

Figure 5. Water Transport in Rotating Disk Reactor.

Disk speeds greater than the 24 rev./min. of run 3 were not attempted since considerable spin-off of liquid was occurring.

In an attempt to improve the reactor performance and decrease the time required to achieve equilibrium conditions, 6 plastic vanes were attached to the disk in the manner of a straight blade fan. Run 4 was then conducted under conditions similar to that of run 2. For run 5 the disk speed was increased to the point of incipient spin-off of liquid (19 rev./min.). Figure 6 is a plot of the ferric ion concentration leaving the reactor as a function of time for these runs. The last run produced the highest conversions for which the last seven data points, averaged to represent "steady-state" operation, gave a value of 63.5 mg Fe^{+3}/l (a yield of 3.56 mg Fe^{+3}/watt-hr.).

In the flowing system used in the rotating disk reactor, fresh Fe^{+2} solution entered the sump and mixed with the partially treated solution. The solution in the sump was conveyed through the corona zone as a thin film on the stainless steel rotating disk. The oxidized solution was then returned to the sump, mixed, and eventually this blended mixture flowed from the system.

After equilibrium in the operation of an ideal single plate flowing system, a constant amount of Fe^{+3} should be produced as a function of time. The data, although somewhat erratic, do show this expected leveling off (Figure 6).

Conclusion

The amount of Fe^{+3} produced per watt-hour in the rotating disk reactor averaged 3.56 with a maximum of 4.45 under the best conditions. In the falling film reactor, an average value of 7.91 was obtained with definite indications that this value could at least be doubled.

Since the efficiency of conversion even with the paddles was less than half that for the falling film reactor and since large reactors employing the rotating disk concept would be more complex and expensive to build and maintain, it was decided, in accordance with the program objectives, to complete the study using the falling film process.

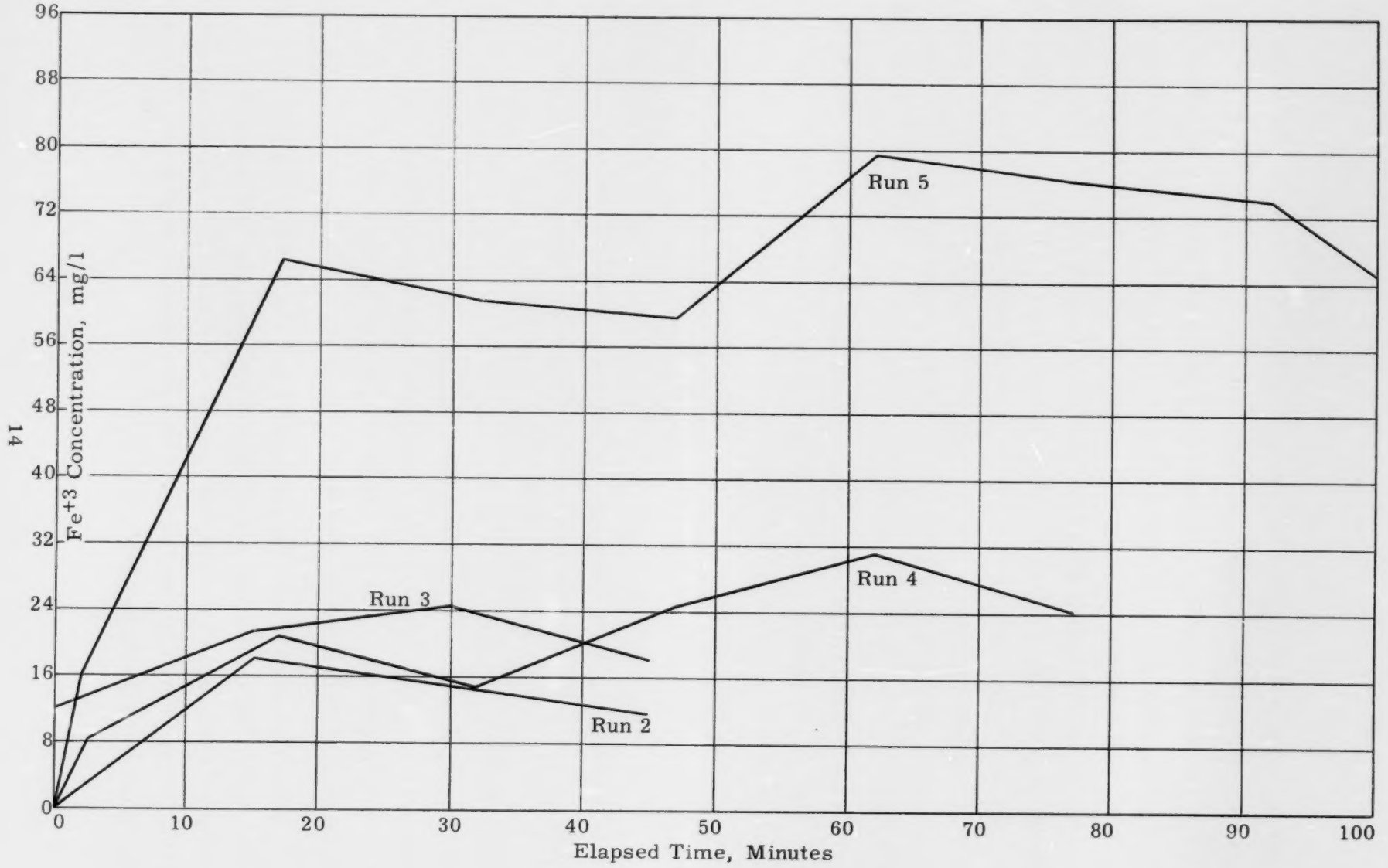

Figure 6. Ferric Ion Concentration Versus Elapsed Time.

(II) DETERMINATION OF PERFORMANCE CHARACTERISTICS FOR FALLING FILM SWIRL REACTOR

Test Objective

The objective of this phase (II) of the program was to determine the optimum relationship between the process variables and the ferrous ion oxidation resulting from corona generated active species in a falling film reactor. An analysis of variance was used to indicate those variables which significantly affected the ferrous oxidation efficiency.

Table I lists the known process variables which were divided into 1) parameters associated with the reactor, and 2) parameters of the process. Those included in the scope of the experiment were randomized or controlled while those not included in the scope were fixed. The table lists 11 variables of which 3 were held fixed throughout the course of the analysis. They include 1) electrode temperature and 2) system pressure, both of which were suspected to be of minor importance in affecting the yield, and 3) the electrode area effect which was beyond the scope of this investigation. Since the limited scope of the study permitted the evaluation of only 2 electrode gap spacings along with the use of either air or oxygen, a series of simple factorial experiments were formulated as follows:

1. The reactor and process were evaluated using air and one electrode gap.
2. The effect of using oxygen and a different electrode gap were each evaluated relative to the air performance.

A simple one-half replicate of a 5 factor orthogonal box design experiment was planned, based on the variables listed in Table II (all other variables fixed). The experiment consisted of 27 runs conducted with each of the controlled variables set at one of five predetermined levels, (Figure 7) where A, B, C, D, and E represented the 5 variables and the subscripts denoted a specific level. Levels 1 and 5 were the minimum and maximum values of that particular variable; level 3 was the mean of range of the variable. Levels

TABLE I

Variables Affecting Reactor Performance

Variable	Assumed Magnitude of effect on yield	Included in scope	Role in Experiment
A. Reactor			
Electrode Gap	small	yes	control
Electrode Area	large	no	fix
Electrode Temperature	small	no	fix
B. Process			
Feed Rate	large	yes	control
Feed Concentration	large	yes	control
Gas Rate			
a. Air	small	yes	control
b. Oxygen	small	yes	control
Gas Humidity	small	yes	control
Power Density	large	yes	control
Pressure	small	no	fix
Analytical Error	small	no	randomize

TABLE II

Operating Range of Variables Analyzed

Variable	Minimum	Maximum
Feed Rate, l/min.	0.250	0.800
Feed Concentration mg Fe^{+2}/l	10.0	150.0
Gas Rate, air ml/min.	25.0	800.0
Gas Humidity, fraction H_2O	0.09	0.75
Power Density, watts/cm^2	0.27	1.8

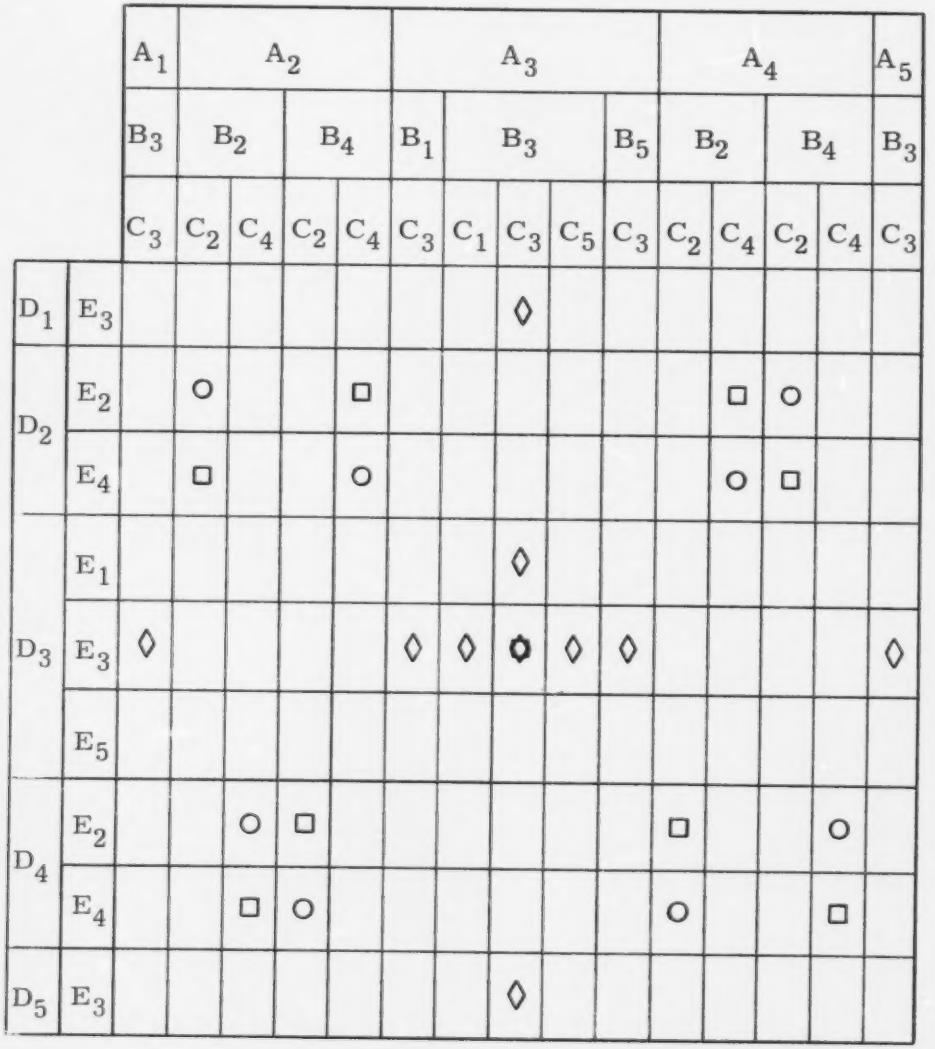

Variables - A, B, C, D, E

Levels - 1, 2, 3, 4, 5

Stage I - ○

Stage II - □

Stage III - ◊

Figure 7. One-half Replicate of a Five Factor Box Design.

2 and 4 were determined from considerations of orthogonality. The experiment was further separated into the three stages. Each stage was run and analyzed before proceeding to the next stage so that significant factors affecting the yield could be recognized and, if necessary, the test plan could be adjusted to encompass the zone of maximum yield. Table III lists the variables, test conditions, and code for relating these to the experimental box design of Figure 7.

Reactor Design

Since the reactor with which the preliminary evaluation runs were made required unwieldly amounts of feed solution a smaller reactor design was selected for this phase of the study, thus enabling a scale of operation compatible with existing laboratory facilities.

A reactor diameter of 3.5 cm was selected (about 3/4 the diameter of the first reactor) with a corona zone of suitable length to provide a liquid residence time similar to that of the larger reactor (0.02 min.) at a flow rate of 0.5 l/min. The length of this zone was calculated using a liquid film thickness that was estimated from a relationship given by W. H. McAdams[12]:

$$B_f = \left[\frac{3\mu_f \Gamma}{\rho_f^2 g}\right]^{1/3}$$

$$\Gamma = \frac{w}{\pi D}$$

where,

B_f = thickness of layer of liquid, ft.
D = diameter, ft.
g = acceleration due to gravity, ft. per hr. per hr.
w = mass rate of flow, lb per hr.
Γ = mass rate per unit breadth, lb per hr. ft.
μ = viscosity of fluid, lb per hr. ft.

TABLE III

Stage I - Values of the Variables and Their Coding

	Variable	Values				
		1	2	3	4	5
A	Feed Rate, l/min	.250	.360	.525	.690	.800
B	Feed Concentration, mg Fe^{+2} /l	10	38	80	122	150
C	Gas Rate, ml air/min	25	179	412	645	800
D	Gas Humidity, fraction H_2O	.09	.22	.42	.62	.75
E	Power Density, watts/cm^2	.27	.57	1.03	1.49	1.8

ρ = density, lb per ft.^{3}

f = subscript for film

At a rate of 0.5 l/min.:

$$w = (0.5)\,(60)\,\left(\frac{1}{28.32}\right)\,(62.4) = 66.1 \text{ lb/hr.}$$

$$\Gamma = \frac{66.1 \times 2.54 \times 12}{\pi \times 3.5} = 183.5 \text{ lb/hr. ft.}$$

$$B_f = \left[\frac{3(2.16)\,(183.5)}{(62.4)^2\ 4.17 \times 10^8}\right]^{1/3} = 1.943 \times 10^{-3} \text{ ft. } (0.0593 \text{ cm}).$$

For a film thickness of 0.0593 cm over the annular surface of the inside wall of the reactor, the volume of solution per centimeter of wall length was:

$$\pi\,(1.55 + 1.49)\,(1.55 - 1.49) = 0.573 \text{ cm}^3$$

where 1.55 was the reactor radius and 1.49 the film radius. Thus, a corona zone of 16 cm. long provided a holdup amounting to 9.17 cm^3 which at a flow rate of 0.5 l/min. gave a residence time of approximately 0.018 min. Figure 8 shows a sketch of this reactor with the pertinent dimensions. The large 34/45 joint at the top provided a means of inserting center electrodes of different diameters for varying the corona gap space. The 19/38 joint vented the non-condensable gases. Feed solution was forced into the reactor through a glass nozzle attached to the 12/30 joint. The liquid jet issued from the nozzle with such velocity that the liquid distributed itself around the circumference of the enlarged section and fell through the corona zone as a thin film on the outer wall. The whole assembly was fabricated from Pyrex glass.

Two center electrodes of Pyrex were fabricated to provide the following operational choices:

Center Electrode Diameter cm	Gap cm	ln Mean Cross-Section Area cm^2
2.5	0.30	140
2.2	0.45	132

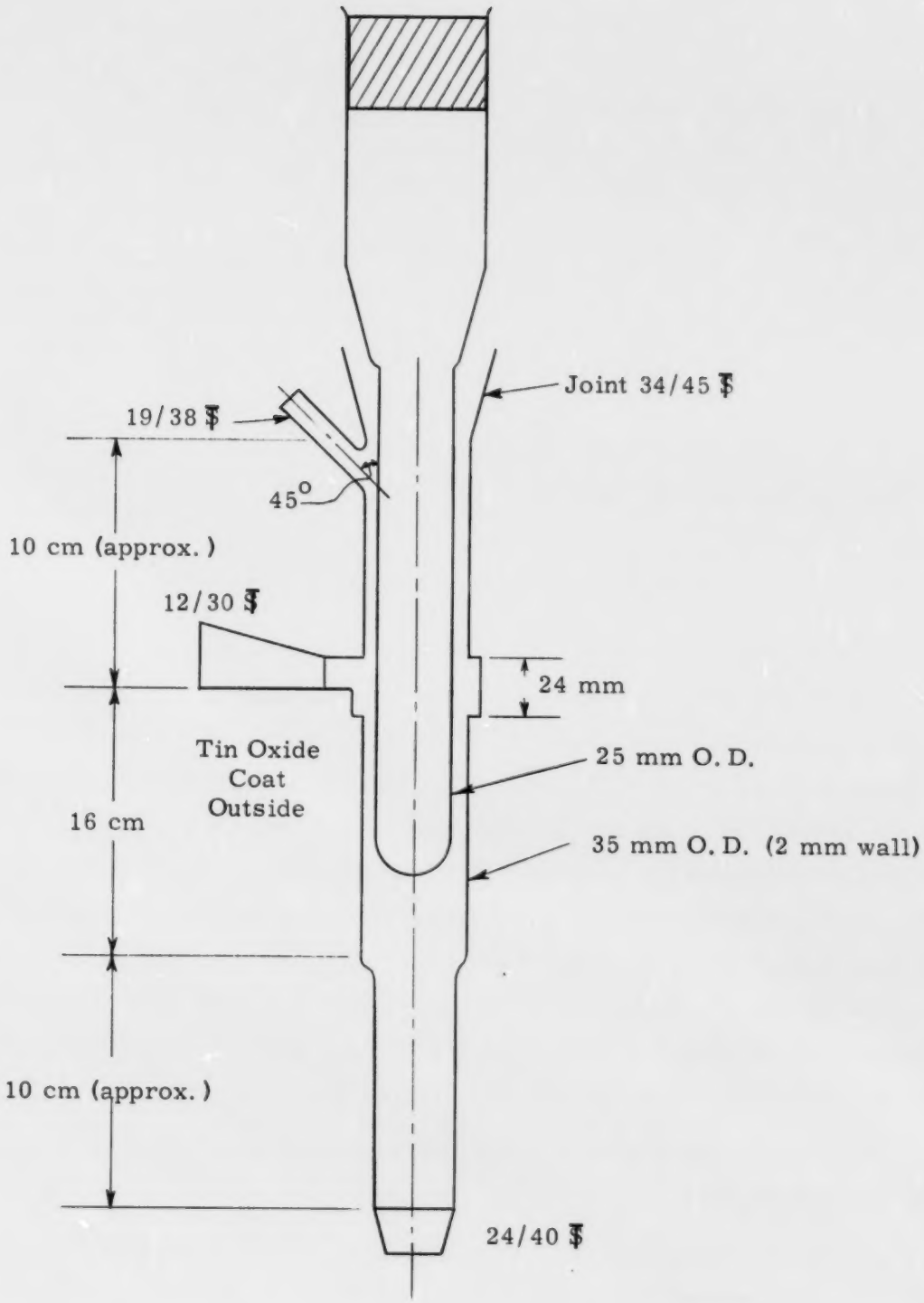

Figure 8. Falling Film Reactor-II.

The feed tank to the reactor had a capacity of approximately 15.1. Appendix A gives the details for preparing the ferrous feed solution.

Operating Procedure

Before introducing air or other gas into the corona zone the water vapor content was adjusted (± 2%) as in the method developed by Hawk, et al.,[9] by saturating the gas with water vapor at some definite temperature. The water in the saturator-boiler was vaporized at any desired rate by adjustment of the energy input to the heating element immersed in the water. Gas passing through the saturator carried with it water in an amount that was dependent on the rate of vaporization, this rate being so regulated that the quantity of water introduced was in excess of that required by the test conditions. The gas-steam mixture then passed into a mixing tube which served to break up the direction of gas flow, facilitating condensation of excess water and helping to equalize the final temperature of the wet-gas mixture. The apparatus was so adjusted that water vapor continuously condensed throughout the length of the tube, and as the gas was always in contact with liquid water, the mixture leaving the top of the apparatus consisted of gas saturated with water at the temperature measured at this point.

When the gas-water vapor mixture had been adjusted to the desired test conditions the liquid flow was started followed by the corona power. After a brief interval the corona stabilized as the center electrode temperature increased. Final flow rate adjustments and power settings were then made. Steady-state operating conditions were reached in about seven minutes; however, operation was continued for three more minutes before samples were collected. For each run two grab samples about 90 seconds apart were taken for analysis. Figure 9 is a flowsheet of the process indicating the major components with their gas and liquid connections.

Variability of the Process

Before beginning the evaluation of the process variables, an experiment

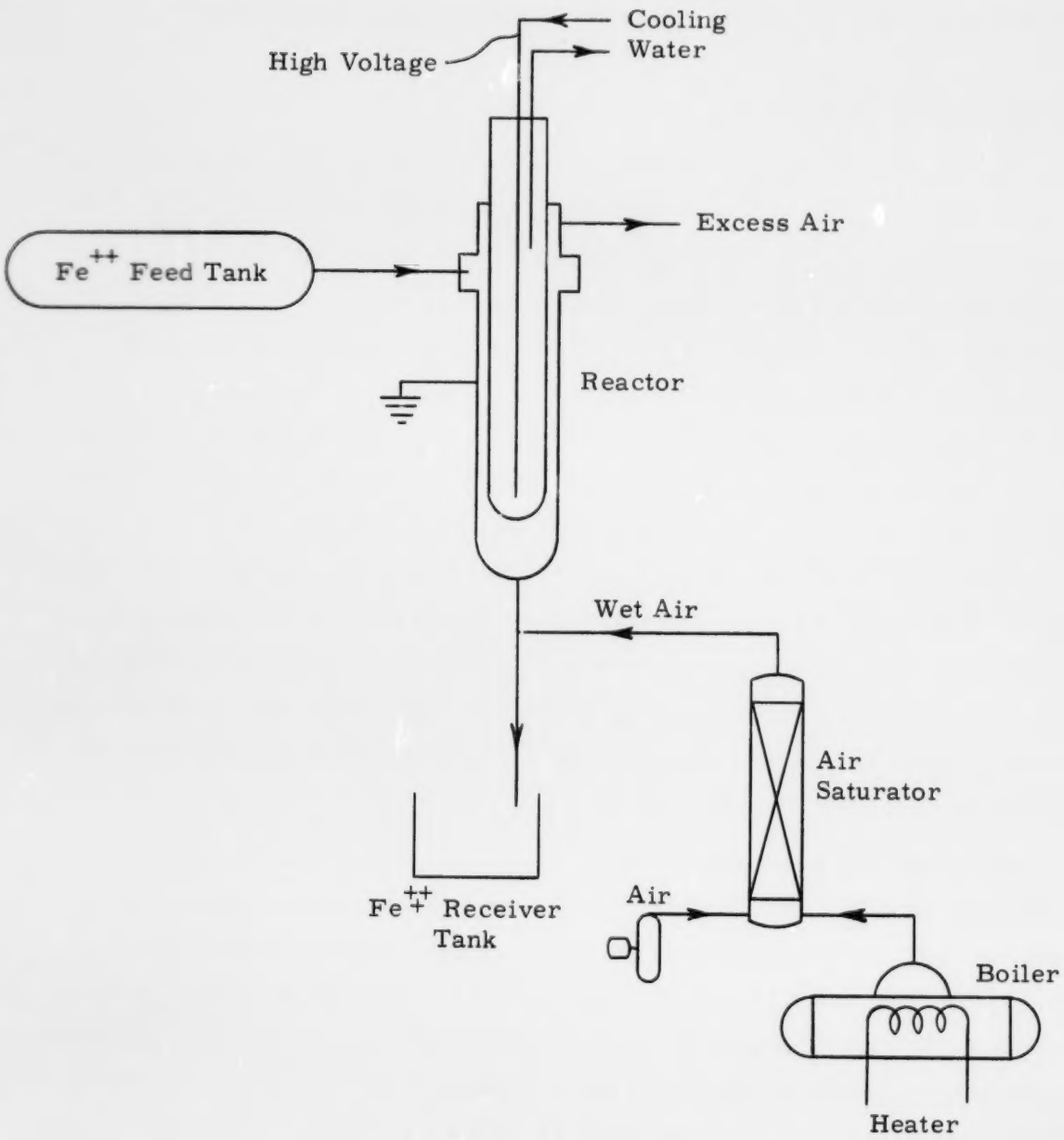

Figure 9. Process Flow Sheet

was conducted to determine the variability between samples during the course of a run. After ten minutes of the corona operation described above, the sampling was started and all solution processed during the next eleven minutes was collected for analysis. The data (Appendix C, Table III) shows the variability between consecutive samples for a typical run. Initially the solution contained 88 mg Fe^{+2}/l. After corona treatment the average value, obtained from five samples that ranged from a low of 75 to a high of 83 mg Fe^{+3}/l, was 80 $\pm$ 1 mg Fe^{+3}/l.

Results of Test

The Stage I data had very poor repeatability, some of the variables were not controlled as originally planned. The two tests which showed the largest differences in yield (3.6 versus 20.8) were actually conducted at similar conditions (see Table IV). The repeat error standard deviation was formally calculated as 6.1 mg Fe^{+3}/watt-hr. Because of this large variability on repeat tests no statistical significance could be found from an analysis of variance. Instead, the averages for each of the conditions were determined (Table IV). Although slightly better average yield were obtained for the "low" feed rate and "high" Fe^{+2} concentration and power density, there was no evidence that these represented more than chance fluctuations. (It turned out that this trend was confirmed in Stage II with respect to feed rate and concentration but not with respect to power density. The tests run on 10/13 and 10/14 gave especially good yields while those on 11/5 were particularly poor. The data, however, were not sufficient to lead to any definite conclusion about a "day-to-day" bias.

The large variability indicates that there were some important variables not being controlled; hence, in an effort to obtain better repeatability and increased yield while using a relatively simple test plan the following changes were made:

1. Increase the range of Fe^{+2} concentration
2. Change the gas rate range
3. Fix the gas moisture content
4. Run electrode cooling water at a temperature of 65 C.

TABLE IV

Stage I - Data Summary /

Run	Date	Level of Variable					Yield, mg Fe^{+3}/watt-hr.					
		A	B	C	D	E						
1	10/14	3	3	3	3	3	15.5	15.3				
2*	10/19,11/2	2	2	2	2	2	10.4	9.9	10.4	5.99	6.12	
3*	11/2,11/4	2	2	4	4	2	5.04	5.11	10.02	10.02		
4*	10/7,10/8	2	4	2	4	4	13.1	11.1	10.5			
5	10/9	2	4	4	2	4	12.5	12.3				
6	11/4	4	2	2	4	4	7.85	7.85				
7	10/20	4	2	4	2	4	5.7	5.3	8.2			
8*	10/9,10/13,11/5	4	4	2	2	2	3.25	3.94	21.3	20.3	3.21	3.42
9*	10/13,11/5	4	4	4	4	2	8.90	17.2	5.96	3.53		

*Run twice

		Average Yield, mg Fe^{+3}/watt-hr. Level - 2	4
A	Feed Rate	10.0	7.6
B	Fe^{+2} Concentration	7.5	10.1
C	Gas Rate (air)	Test conditions not achieved	
D	Gas Moisture	9.0	8.6
E	Power Density	7.9	9.7

Notes:

/ Raw data listed in Table IV of Appendix C.

These changes simplified the test plan. There were now four variables run at two levels each, with four runs duplicated. The revised test plan was a 2^4 factorial test in two stages. Table V shows this revised Stage II test plan, the variables, test conditions, and yields obtained. An analysis of variance of yield (Table VI) led to the following conclusions:

1. Feed concentration was found to be by far the most important variable (significant at 1% statistical level). The average yield was 23.5 at the high Fe^{+2} level versus 9.9 at the low Fe^{+2} level.

2. Gas rate was the second most important variable (significant at a 1% statistical level). The average yield at the high flow rate was 20.7 versus 12.8 at the low flow rate.

3. Feed rate and power density were also both found statistically significant (at a 5% level). Yield tended to increase with decrease in feed rate and with decrease in power density.

4. There is evidence of significance (at the 5% statistical level) with respect to at least one of the following interaction pairs:

   a. Fe^{+2} concentration - gas rate (suggesting the importance of simultaneously having high concentration and high gas rate).

   b. Feed rate - power density (suggesting the importance of simultaneously having low feed rate and low power density).

   With these limited tests it was not possible to distinguish between the above two interactions.

5. The experimental error standard deviation for yield was estimated from repeat tests to be 1.8 mg Fe^{+3}/watt-hr.

Experimental error in this stage of the test program was greatly reduced from the previous stage and it was possible to detect significant differences with respect to each of the variables. Table VII compares the averages for

TABLE V

Revised Stage II - Plan and Data Summary /
(1/2 2^4 fractional factorial)

Run	Date	Level of Variable					Yield, mg Fe^{+3}/watt-hr.			
		A	B	C	D	E				
1*	11/11	2	2	2	2	2	15.1	16.1	13.8	12.5
2*	11/11	2	2	4	2	4	7.6	8.8	8.9	8.5
3	11/13	2	4	2	2	4	19.2	18.8		
4	11/13	2	4	4	2	2	33.3	35.5		
5	11/12	4	2	2	2	4	3.02	3.09		
6	11/12	4	2	4	2	2	14.8	12.3		
7*	11/12,11/13	4	4	2	2	2	19.0	14.0	17.1	8.04
8*	11/12,11/13	4	4	4	2	4	25.7	25.1	26.3	27.8

*Run twice

Test Values of the Variables

		Level 2	Level 4
A	Feed Rate, l/min.	.360	.690
B	Feed Concentration, mg Fe^{+2}/l	80	160
C	Gas Rate, ml air/min.	790	1530
D	Gas Humidity, fraction H_2O	.22	.22
E	Power Density, watts/cm^2	.57	1.49

Notes:

/ Raw data listed in Table V of Appendix C.

TABLE VI

Stage II - Analysis of Variance with Respect to Yield

	Variable	Degrees of Freedom	Mean Square	F Ratio	Statistical Significance
A	Feed Rate	1	44.7	14.4	5%
B	Fe^{+2} Concentration	1	371.3	119.8	1%
C	Gas Rate	1	125.6	40.5	1%
E	Power Density	1	50.5	16.3	5%
	AB = CE	1	5.3	1.7	NS
	AC = BE	1	20.2	6.5	10%
	AE = BC	1	63.3	20.4	5%
	Error	4	3.1		

TABLE VII

Comparison of Stage I and Stage II Average Yield
(mg Fe^{+3}/watt-hr.)

	Variable	Stage I		Stage II	
		Low Level	High Level	Low Level	High Level
A	Feed Rate	10.0	7.6	19.1	14.4
B	Fe^{+2} Concentration	7.5	10.1	9.9	23.5
C	Gas Rate	---	---	12.8	20.7
D	Gas Moisture	9.0	8.6	--	--
E	Power Density	7.9	9.7	19.2	14.2

Stage I and Stage II data showing the improvement in yield from adjustment of the test conditions.

Further adjustment of the range of the test variables could be made for purposes of improving the yield, or the interaction between the variables could be obtained as an aid in characterizing the reactor performance. The latter plan was chosen as probably being better able to provide the most information in the limited scope of this program. Accordingly, the other half of the 2^4 factorial plan was conducted. The actual test plan was very similar to that of the Stage II; the only difference was the interchange of levels for the E variable. Table VIII shows this new Stage III plan and the yields obtained.

The 16 tests of the Stage II and Stage III plans completed a statistical 2^4 factorial experiment, with each of the four variables considered at two levels - supplemented by seven repeat tests.

Combined analyses of variance were conducted to evaluate the statistical significance of the relationships between the process variables, yield, (Table IX) and percent conversion (Table X). The averages for each of the variables and those for the apparently more important interactions were also determined and are shown for yield and percent conversion in Tables XI and XII, respectively. The results are given in least squares regression form in Table XIV. An additional analysis of variance to evaluate repeatability is shown in Table XIII.

Examination of the Tables IX to XIII led to the following conclusions:

A. With respect to yield:

1. Concentration was the only variable found statistically significant (at the 5% significance level). Average yield at 160 mg Fe^{+2}/l was 22.4 units versus 10.1 units at 80 mg Fe^{+2}/l.

2. Appreciably higher yields were found for <u>simultaneous</u> exposure to both low feed rate and low power input than to any of the other three combinations of conditions. These

TABLE VIII

Revised Stage III Plan and Data ††

Run	Date	Level of Variable †					Yield, mg Fe^{+3}/watt-hr.			
		A	B	C	D	E				
9	11/23	2	2	2	2	4	9.48	9.48		
10	11/23	2	2	4	2	2	21.6	22.2		
11*	11/27,11/30	2	4	2	2	2	47.4	47.4	24.9	25.4
12	11/27	2	4	4	2	4	18.8	18.8		
13	11/24	4	2	2	2	2	6.02	5.27		
14	11/25	4	2	4	2	4	4.55	3.94		
15*	11/27	4	4	2	2	4	6.76	8.62	37.1	37.4
16	11/27	4	4	4	2	2	4.67	3.84		

*Run twice

Notes:

†. Test values of the variables same as those of Table V

††. Raw data listed in Table VI of Appendix C

TABLE IX

Combined Analysis of Variance For Yield

		Degrees of Freedom	Mean Square	F Ratio	Statistical Significance
A	Feed Rate	1	111.8	1.44	NS
B	Fe^{+2} Concentration	1	618.8	8.89	5%
C	Air Rate	1	56.6	<1	NS
E	Power Density	1	131.7	1.89	NS
AB		1	11.1	<1	NS
AC		1	.1	<1	NS
AE		1	73.5	1.06	NS
BC		1	.1	<1	NS
BE		1	13.1	<1	NS
CE		1	13.1	<1	NS
Higher Order Interactions /and Repeats		12	69.6		

Estimated standard deviation measuring repeatability of yield = 8.3

TABLE X

Combined Analysis of Variance For Conversion

	Degrees of Freedom	Mean Square	F Ratio	Statistical Significance
A = Feed Rate	1	10998.8	38.0	1%
B = Fe^{+2} Concentration	1	215.4	<1	NS
C = Air Rate	1	362.0	1.4	NS
E = Power Density	1	2467.6	9.3	5%
AB	1	907.5	3.4	10%
AC	1	0	0	NS
AE	1	77.0	<1	NS
BC	1	1.4	<1	NS
BE	1	822.3	3.1	10%
CE	1	47.3	<1	NS
Higher Order Interactions /and Repeats	12	265.8		

Estimated standard deviation measuring repeatability of conversion = 16.3

TABLE XI

Average Yields

Single Parameter, units as noted		Yield, Mg Fe^{+3}/watt-hr
Feed Rate (l/min)	0.360	19.0
	0.690	13.7
Concentration (mg Fe^{+2}/l)	80	10.1
	160	22.5
Gas Flow Rate (cm^3/min)	790	14.4
	1530	18.2
Power Density (watts/cm^2)	0.57	19.2
	1.49	13.5

Interactions (Two Parameters)

Feed Rate (l/min)	Power Density watts/cm^2	Yield mg Fe^{+3}/watt-hr
0.360	0.57	24.0
0.360	1.49	14.0
0.690	0.57	14.4
0.690	1.49	13.0

Concentration mg Fe^{+2}/l	Gas Flow Rate cm^3/min	Yield mg Fe^{+3}/watt-hr
80	790	8.8
80	1530	11.0
160	790	16.7
160	1530	30.3

Average Yield Stage I: 16.7 mg Fe^{+3}/watt-hr

Average Yield Stage II: 15.8 mg Fe^{+3}/watt-hr.

TABLE XII

Average Conversion

Single Parameter, units as noted		Conversion, percent
Feed Rate (l/min)	0.360	83.1
	0.690	30.7
Concentration (mg Fe^{+2}/l)	80	53.3
	160	60.6
Gas Flow Rate (cm^3/min)	790	52.2
	1530	61.7
Power Density (watts/cm^2)	0.57	44.5
	1.49	69.3

Interactions, (Two Parameters)

Concentration mg Fe^{+2}/l	Power Density watts/cm^2	Conversion percent
80	0.57	48.0
80	1.49	58.5
160	0.57	41.0
160	1.49	80.0

Concentration mg Fe^{+2}/l	Feed Rate l/min	Conversion percent
80	0.360	87.0
80	0.690	19.5
160	0.360	79.3
160	0.690	41.9

Average Conversion Stage I: 56.9 percent

Average Conversion Stage II: 56.9 percent

TABLE XIII

Evaluation of Fe^{+2} to Fe^{+3} with Respect to Repeatability

Analysis of Variance for Yield, mg Fe^{+3}/l

Source of Variation	Degrees of Freedom	Mean Square	"F" Ratio	Statistical Significance
Between Stages	10	83.1	51.9	1%
Within Stages	2	1.6		

Analysis of Variance for Conversion, percent

Source of Variation	Degrees of Freedom	Mean Square	"F" Ratio	Statistical Significance
Between Stages	10	267.0	7.9	1%
Within Stages	2	33.7		

variables and their interactions had been found significant in the earlier stage (II) of the experiment and the final results were very similar in magnitude. However, for Stage III they were no longer statistically significant because of increased experimental error (see below).

3. In Stage II of the experiment an air rate of 1530 ml/min produced appreciably higher yields than that of 790 ml/min. In the last stage (III) of the program, essentially identical results were obtained at these two conditions. Although the overall results still slightly favored the higher air rate, a statistically significant difference was not obtained.

4. The average yield in the two stages (II and III) were very similar and a statistically significant difference did not occur between them.

5. The experimental error standard deviation for yield was estimated, after the elimination of a number of doubtful values which exhibited considerable discrepancy from repeat tests, at 8.3 Fe^{+3}/watt-hr. Repeatability was appreciably poorer in Stage III of the program than in the previous Stage II because of the variability at a few conditions (such as run numbers 15 and 16). The variability between repeat samples from different batches was significantly larger than that for samples from the same batch (Table XIII). This difference could, however, be due to a time factor rather than actual batch differences. Because of poor repeatability, it was difficult to establish statistical significance for the experimental variables (Table II) under study.

B. With respect to percent conversion:

1. Feed rate was by far the most important variable (significant at the 1% statistical level). Percent conversion at 0.360 l

Fe^{+2}/min. was 83.1% versus 30.7% at 0.690 l Fe^{+2}/min.

2. Power input was the second most important variable (significant at the statistical 5% level). Percent conversion at 1.49 watts/cm^2 was 69.3% as compared to 44.5% at 0.57 watts/cm^2.

3. The main effect of concentration was not statistically significant. However, there was some evidence of interaction between both concentration and feed rate and between concconcentration and power input. In particular, higher percent conversions were associated with high concentration in conjunction with feed rates of 0.690 l Fe^{+2}/min. and power inputs of 1.49 watts/cm^2. In contrast, slightly higher percent conversions were obtained at the low concentration than at the high concentration for feed rates of 0.360 l/Fe^{+2}/min. and power inputs of 0.57 watts/cm^2.

4. There was no significant effect of air rate on percent conversion. Slightly higher average percent conversion, however, was obtained at an air flow rate of 1530 ml/min. than at an air flow rate of 790 ml/min.

5. Identical <u>average</u> values of percent conversion were attained in Stages II and III of the experiment.

6. The experimental error standard deviation for percent conversion was estimated as 16.3%. This is again indicative of appreciably poorer repeatability in Stage III of the program as compared with that in Stage II. As was the case for yield, significantly larger variation was found on repeat tests from different batches as compared to repeat tests from the same batch.

Least squares regression functions were fitted to the results of the experiment as shown in Table XIV. These functions included only linear and

TABLE XIV

Least Squares Regression Equation

CODE

Y_1 = Yield (mg Fe^{+3}/watt-hour)

Y_2 = % Conversion

$$X_A = \frac{\text{Feed Rate} - 0.525}{0.165} \quad (1\ Fe^{+2}/\text{min.})$$

$$X_B = \frac{\text{Concentration} - 120}{40} \quad (\text{mg } Fe^{+2}/1)$$

$$X_C = \frac{\text{Air Rate} - 1160}{370} \quad (\text{ml/min.})$$

$$X_E = \frac{1.12\ (\text{Power Density}) - 1.15}{0.51}$$

Equation for Yield

$$Y_1 = 16.3 - 2.64X_A + 6.22X_B - 2.87X_E + 2.14X_A X_E$$

Equation for % Conversion

$$Y_2 = 56.9 - 26.22X_A + 3.67X_B + 4.76X_C + 12.42X_E + 7.51X_A X_B + 7.17X_B X_E$$

Standard Error (True Yield)

$$= 8.3 \left[\frac{1}{16}\left(X_A^2 + X_B^2 + X_E^2 + X_A^2 X_E^2 + 1\right)\right]^{1/2}$$

Standard Error (Future Observation for Yield)

$$= 8.3 \left[\frac{1}{16}\left(X_A^2 + X_B^2 + X_E^2 + X_A^2 X_E^2 + 17\right)\right]^{1/2}$$

Standard Error (True % Conversion)

$$= 16.3 \left[\frac{1}{16}\left(X_A^2 + X_B^2 + X_C^2 + X_E^2 + X_A^2 X_B^2 + X_B^2 X_E^2 + 1\right)\right]^{1/2}$$

Standard Error (Future Observation for % Conversion)

$$= 16.3 \left[\frac{1}{16}\left(X_A^2 + X_B^2 + X_C^2 + X_E^2 + X_A^2 X_B^2 + X_B^2 X_E^2 + 17\right)\right]^{1/2}$$

interaction terms and represented only an approximation of the true underlying relationship between the process variables, yield, and percent conversion. Certainly the expressions were applicable only within the range of experimentation.

The standard deviations shown provide measures of the precision of the equation for predicting the true value at a particular condition, and for predicting a single future observation from the given equation.

Oxygen and Electrode Gap Tests

A simple eight run test plan was prepared for comparing the effect of using oxygen in place of air in the corona zone and evaluating the effect of changing the electrode gap spacing. Table XV shows this plan and data for the first four runs. From these meager data it appears that the oxygen was less than half as efficient as air for the ferrous-ferric conversion and that increasing the electrode gap lowered the yield in the case of oxygen but had little effect in the case of air operation. The balance of the runs were not completed at the direction of the contracting officer.

Miscellaneous Tests

Three other tests were run to determine 1) the amount of oxides of nitrogen present in the corona treated iron solution, 2) the effect of running in an inert gas atmosphere, and 3) a test to determine the effect of doubling the ferrous ion concentration over the 170 mg/l value used in the factorial tests. The test conditions employed and results obtained are given in Table VIII of Appendix C.

The first run was conducted under conditions similar to those of run 15 (Table VIII) and like results were obtained; the yield value was 33 units and conversion 92%. The oxides of nitrogen found amounted to 5.3 mg NO_3/l. Thus, a nitrogen-oxygen reaction occurred in the corona zone.

For the second run under an argon atmosphere, the test conditions were similar to those of run 15 except that it was not possible to run the power density

TABLE XV

Oxygen and Electrode Gap Test Plan and Data Survey /

Run	Feed Concn. mg/l	Feed Flow Rate l/min	Gas	Gas Flow Rate cm^3/min.	Power Density watts/cm^2	Gap cm.	Yield mg Fe^{+3}/watt-hr	
1	160	.360	O_2	1530	.57	.30	11.7	10.6
2	160	.360	O_2	1530	.57	.45	6.4	7.4
3	160	.360	air	1530	.57	.30	25.4	29.3
4	160	.360	air	1530	.57	.45	39.2	24.0
5	80	.690	O_2	790	1.49	.30	-	-
6	80	.690	O_2	790	1.49	.45	-	-
7	80	.690	air	790	1.49	.30	-	-
8	80	.690	air	790	1.49	.45	-	-

/ Raw data listed in Table VII of Appendix C.

above 0. 55 without endangering the reactor from an arc-over which would puncture the electrode. A yield of 6 mg Fe^{+3}/watt-hr. with a conversion of 6. 5% was obtained. These values were lower even than those obtained with oxygen but they did show that certain active species were generated in the water vapor atmosphere of the corona zone.

The third run, using 332 mg Fe^{+2}/l feed solution, gave a yield of 43 mg Fe^{+3}/watt-hr with a 67% conversion. The regression equation while unreliable at this concentration predicted a yield value of 46. The performance tests showed a great dependence of yield upon concentration and apparently this trend continued through 330 mg Fe^{+2}/l.

(III)ORGANIC OXIDATION

Public Health Service Tests

A variety of solutions containing organic materials were run through the corona reactor by Public Health Service personnel and examined for their change in oxygen demand. Table IX of Appendix C lists these runs, test conditions, and results obtained (analytical method given in Appendix B).

Both air and oxygen were compared for the COD reduction of benzoic acid solution and as with the ferrous tests the best results were obtained from the use of air.

The study was conducted on aqueous solutions of benzoic acid and alkyl benzene sulfonate, filtered secondary effluents, and effluents from a carbon adsorption column. Distilled water was used as a control and to rinse the reactor before and after use of a new test solution.

The reactor was operated at three power levels; 80 watts, 144 watts, and 210 watts. The reduction in COD per pass through the reactor averaged about 2 mg/l for all organic oxidation experiments. Because of the small change in COD, the effects of concentration of the organics on the oxidation efficiency could not be reliably evaluated. The best oxidation efficiencies occurred at

the lowest power level (80 watts Table III) averaging about 58 kwh per 1000 gallons for a 10 mg/l reduction in COD. The best oxidation efficiency at the 80 watt power level was 27.5 kwh per 1000 gallons.

TABLE XVI

Corona Oxidation

Power Level: 80 watts Liquid feed rate: 0.36 liters/min

System	Initial COD	ΔCOD	meq/watt-hr	kwh/1000 gal/10 COD
Benzoic Acid	20.4	2.2	0.075	63.7
Benzoic Acid	195.0	3.8	0.129	36.9
Benzoic Acid	33.5	1.1	0.037	127.0
ABS	22.1	3.0	0.100	46.7
ABS	21.7	3.5	0.119	40.1
Secondary Eff. I	75.6	0.2	0.014	700.0
Eff.I and H_2O	36.4	1.5	0.050	93.5
Secondary Eff.II	72.2	5.1	0.170	27.5
Eff. II and H_2O	36.1	--	--	--
Carbon Eff.	2.0	1.4	0.047	100.0
		Average power: kwh/1000 gal/10 COD		58.0

Contrary to reports in the literature, hydrogen peroxide was not detected in the distilled water runs. Apparently the hydroxyl radical transport from the gas phase to the liquid phase did not occur in quantities sufficient to produce measurable hydrogen peroxide concentrations in distilled water. The life of the active oxygen species (·OH, O) may be too short to allow appreciable diffusion transport of these species from the gas phase to the liquid phase.

A possible effect of concentration on the efficiency of COD reduction was indicated in the treatment of secondary effluents:

Average initial	COD mg/l	Δ COD mg/l
	75.9	4.26
	36.2	2.66
	22.3	0.15

where high concentration of oxidizable materials gave the greater conversions. Power requirements for the high COD solutions were about 1 Δ COD/watt-hr at a flow rate of 0.36 l/min. (5.7 gal./hr.). Successive passes of the corona treated solution through the reactor appeared to be of minor value in changing the COD value; the largest change occurred in the first four passes with very little additional change occurring after nine passes. With each successive passage through the reactor the solution became hotter. It was likely that this warm solution dislodged material which contributed to the overall COD thus masking the small reduction in COD per pass through the reactor.

Corona treatment of ABS solutions gave COD reductions of about 9% with 55% loss of the ABS concentration (as determined by the methylene blue Helige comparator method).

(IV) ECONOMIC CONSIDERATIONS

Before consideration of the preliminary economic estimate for the costs of equipment to produce 10 mg/liter and 100 mg/liter of available active oxygen COD for advanced waste treatment plants ranging from one million to 100 million gallons per day, it is necessary to describe briefly the type and function of the several components of a corona process equipment. These include a power supply with associated control equipment and a corona reactor.

The power supply for a corona reactor consists of:

a. Motor-generator set
b. High voltage transformer
c. Tuning circuit (choke and/or capacitors)
d. Control and instrumentation

The ratings for the power supply are dependent upon the characteristics of the corona reactor and the load which it presents to the power supply. The details of corona reactor construction which affect the power supply ratings are:

a. Corona power required
b. Electrode corona power density
c. Gas and material reacted
d. Gas or electrode gap
e. Electrode dielectric barrier material

With these parameters specified, it is possible to determine:

a. Peak voltage required to initiate corona
b. Barrier thickness required to withstand the total voltage across the barrier in the event of an arc across the gas
c. Dielectric barrier, gas, and total reactor capacitance
d. Maximum operating voltage
e. Capacitive (charging) current drawn by the reactor
f. Corona (resistive) current drawn by the reactor
g. Resultant load current drawn by the reactor
h. Power factor of the corona reactor load

Motor-Generator Set

The KVA rating of the motor-generator set is determined by the product of the corona operating voltage and the resultant load current (or, the corona power divided by the power factor). Experience at ATL indicates that the optimum frequency for a large scale corona process is about 10,000 cycles per second. This conclusion was reached by balancing the experimental observation that the corona power generated in a gaseous gap in series with a dielectric is directly proportional to frequency. Above 10,000 cycles per second, high frequency power becomes too costly, while below 10,000 cycles per second the lower frequencies require higher voltages or increased corona

reactor capacitance. The output voltage of the generator can be any value consistent with usual generator practice and with the transformer primary voltage.

High Voltage Transformer

The KVA rating of the high voltage transformer will usually be the same as that of the motor-generator set. The secondary voltage will be determined by the corona reactor requirements for voltage breakdown of the gaseous gap. Secondary or load current will be the vector sum of charging current and resistive or corona current. Primary voltage must be consistent with generator output voltage. If experimental flexibility is required, the transformer can be arranged for series or parallel connection.

Tuning or Power Factor Correction Circuit

If the corona reactor load results in a poor power factor, there are two possible means of solution: 1) the motor-generator set must be built with sufficient KVA capacity to meet the power factor and corona power requirements; or 2) the secondary circuit of the transformer and the corona reactor can be tuned with a parallel resonant circuit consisting of a tuning choke and high voltage capacitors, or with a series resonant circuit consisting of a tuning choke and the corona reactor load capacitance.

The decision as to whether the motor generator should be built with increased capacity or whether the secondary circuit should be tuned would be based on economic considerations. In general, the dollars per KVA are higher for motor generator sets than for tuning circuit components.

Control and Instrumentation

Control and instrumentation equipment for a corona reactor power supply must include:

a. Provision for varying transformer output high voltage from zero to maximum. (This can be done by varying generator field current.)

b. Provision for measuring generator output (and thus, transformer input) voltage, current, and power.

c. Provision for measuring the peak high voltage applied to the corona reactor.

d. Provision for measuring the corona reactor power.

e. A current overload relay for removing high voltage from the corona reactor in the event of a short circuit in the reactor, or a low voltage, high current arc across the electrodes.

Corona Reactor

The actual design of the corona reactor is dependent upon a number of variables such as reactor type, operating voltage, construction materials, dimensions and geometry, etc., and the costs could vary considerably, particularly since the dielectric barrier materials are very expensive. There are, however, a number of factors common to all corona reactor designs which permit scaling up the costs of a large size reactor.

Costs

Since the proposed plant would be in the range considerably above 1,000 KW, the corona generating equipment would consist of a number of basic package units in the 1250 to 1500 KW range. Scale-up of equipment has never been attempted on the scale required, and the generating equipment would have to be designed and fabricated as a special unit. During the course of design, new ideas and concepts undoubtedly will be originated so that at present it is impossible to give a more detailed description.

The costs presented are those for the corona reactor and for those major items of special equipment to generate and control the high voltage, high frequency power applied to the corona reactor. No attempt has been made to factor in such items as return on capital investment, depreciation, cost of site or building, cost of purchased power, which vary considerably, or many

of the other numerous items which are common to any large electrical installation.

The projected costs are based upon ferrous oxidation half reaction

$$Fe^{+2} \rightarrow Fe^{+3} + e^{-}$$

and the reactor performance data which differ according to whether or not nitrogen is present, from Appendix C, the following yield values are typical:

with N_2	40	mg Fe^{+3}/watt-hr
excluding N_2	10	mg Fe^{+3}/watt-hr

For ferrous oxidation equivalents equal to 10 mg/l of COD, the amount of Fe^{+2} oxidized is

$$\frac{55.85 \times 10}{8} = 69.9 \text{ mg/l}$$

and for 100 mg/l of OH the amount of Fe^{+2} oxidized equals 699 mg/l. Then the power required to generate the oxidizing species for these different conditions is:

COD mg/liter	Power, watt-hr/liter	
	With N_2	Without N_2
10	1.75	6.99
100	17.5	69.9

For example, the power required to provide 10 and 100 mg/l COD in processing plants handling 10^6 or 10^8 gal./day are shown in Table XVII.

Based on these power estimates, the range of KW is such that the overall plant project can be interpreted as a multiplicity of individually rated high voltage, high frequency power supplies of 1250 to 1500 KW capability per unit. The cost per kilowatt for such a unit would be approximately the same over the spread of KW above. While the output might vary with the load power factor, a 1500 KW generator can be assumed to generate about 1250 KW of corona power.

TABLE XVII

Estimated Power Requirements For Providing COD in Liquid Wastes

Case With N_2

COD Concentration mg/l	KWH/1000 gal.	Gal. 24 hr. day	Kilowatts
10	6.62	10^6	275
		10^8	27,500
100	66.2	10^6	2,750
		10^8	275,000

Case Without N_2

10	26.5	10^6	1,100
		10^8	110,000
100	26.5	10^6	11,000
		10^8	1,100,000

The following major equipment costs are on the basis of dollar per kilowatt of motor-generator output power.

Description	$ per KW
Drive motor and 1500 KW, 10 KC generator	130
High and Low Voltage bus bars and disconnect switches	25
High Voltage Transformer	10
Tuning Reactor	5
Control and Instrumentation	10
Total	180
Total (with installation)	225
Reactor alone (installed)	85
TOTAL	310

From this cursory analysis it appears that a plant to process 1 mgd requiring 10 mg/l COD would cost between $\$4 \times 10^4$ to $\$16 \times 10^4$ and a 100 mgd plant one hundred times as much as the 1 mgd. The estimated cost for similar plants producing 100 mg/l COD would range from $\$4 \times 10^5$ to $\$16 \times 10^5$ for treating 1 mgd with a hundred-fold increase for a 100 mgd plant.

SUMMARY OF THE FOUR PROJECT PHASES

The superior performance of the falling film swirl reactor over the rotating disk reactor was due to several different factors. Poor wetting of the stainless steel disk induced a loss of efficiency in transporting material through the corona zone over that of the falling film in which all of the material passed through the corona zone. At the lowest disk speed used, 4 rev./min., all of the liquid feed should have passed through the corona zone over three times had there been good mixing and transport of liquid. The addition of paddles to the disk and increasing the disk speed produced only minor gains in efficiency, obviously the rotating disk failed to perform as predicted.

Evaluation of the variables which affected the performance of the falling film reactor was subject to a number of unexpected variations with the result

that only the first order of effects and their interactions were determined. Within the program scope, it was not possible to determine the causes of the variations which continued even though strict adherence to operating procedures was followed. The large experimental error indicated that there were other unknown variables which were not under control. The strong effect of concentration on the Fe^{+++} yield indicated that the diffusion of corona generated active species from the gas into the liquid was the rate controlling step in the process and that means of increasing the liquid surface exposed to the corona are required to improve this diffusion.

Operation of the reactor in an oxygen or inert gas atmosphere greatly reduced the ferrous conversion over that of air operation. Thus, unfortunately, the oxides of nitrogen appeared as important reacting species. Analysis for nitrates, however, gave values which were insufficient to account for the conversions obtained. Nitrite, and other intermediate oxidation states of nitrogen, may have been the primary corona generated material responsible for the ferrous-ferric conversion. However, project limitations did not permit this point to be definitely established.

The importance of active nitrogen-oxygen species was given added support by the low conversions obtained when aqueous organic media were treated in the reactor. While ferrous was easily oxidized, such materials as benzoic acid, alkyl benzene sulfonate, and sewage effluents required relatively active oxidants.

Ferrous ion is also oxidized by atomic hydrogen[2,5]. The presence of such species in the reactor could arise from the decomposition of water; however, any such effect is small by comparison with the observed nitrogen reaction. Radiolysis chemistry[1] predicts the presence of hydrogen peroxide, and Hickling and co-workers[4,6,10] claim to have generated a substantial amount using a similar ferrous sulfate solution in a static system under reduced pressure with a d-c corona discharge; however, in our investigation, qualitative tests using the titanic acid reagent failed to respond to both the

liquid and gaseous effluent from the swirl reactor.

The average power requirement of 58 kwh per thousand gallons per 10 mg/l of COD for organic oxidation in water with air or oxygen atmospheres and at the most effective (80 watt) power level was greater than the power requirements of 6.6 and 26.5 kwh per thousand gallons per 10 mg/l of COD for, respectively, the air-ferrous and oxygen-ferrous oxidation systems. Although the small changes in COD of the various organic substrate per pass through the reactor reduced the reliability of the organic oxidation power requirement, the high average power requirement qualitatively indicated that the easily oxidized ferrous ion reacted with corona activated species which did not strongly attack the various organic substrates.

Because of the limited project scope, the effect of the concentration of organic molecules compared to ferrous ions, the interaction of the various oxidizable substances with the corona activated species, the identification of the corona species, and the quantitative effect of interphase surface area on the oxidation efficiency were not determined. In addition, the limited scope, unfortunately, did not permit additional organic studies at the longer contact time needed to reduce COD analytical variability and did not permit redesign of the reactor system for improvement in interphase surface area.

For the rotating disk and the falling film reactor and with corona power costs between one and two cents per kwh, however, even at the lower oxidation power requirements of the ferrous oxidation system, corona treatment of waste waters was not economical.

ACKNOWLEDGEMENTS

The authors wish to acknowledge the contribution of W. T. Doyle who performed all of the iron analyses. They also wish to recognize the assistance of D. F. Bishop, Project Officer for this contract at the R. A. Taft Sanitary Engineering Center, Cincinnati, Ohio.

REFERENCES

1. Allen, A. O., The Radiation Chemistry of Water and Aqueous Solutions, D. VanNostrand Co., Inc., Princeton, N.J., 1961.

2. Czapski, G., and G. Stein, "Oxidation of Ferrous Ion in Aqueous Solution by Atomic Hydrogen," Nature 182, 598 (1958).

3. Cobine, J. D., Gaseous Conductors, Dover Publications, Inc., New York, New York 1958.

4. Davies, R. A., and A. Hickling, "Glow-discharge Electrolysis. Part I. The Anodic Formation of Hydrogen Peroxide in Inert Electrolysis," J. Chem. Soc., 3595 (1952).

5. Davis, T. W., Gordon, S., and Hart, E. J., "Chemical Effects of Atomic Hydrogen in Aqueous Solutions," J. Am. Chem. Soc. 80, 4487 (1958).

6. Denaro, A.R., and Hickling, A., "Glow-discharge Electrolysis in Aqueous Solutions," J. Electrochemical Soc. 105, 265 (1958).

7. Devins, J. C., and Sharbaugh, A.H., "The Fundamental Nature of Electrical Breakdown," Electro-Technology 70, 103 (1961).

8. Hart, E. J., "The Hydrated Electron," Science 146, No. 3640, 19 (1964).

9. Hawk, C.O., Golden, P.L., Storch, H.H., and Fieldner, A.C., "Conversion of Methane to Carbon Monoxide and Hydrogen," Ind. Eng. Chem. 24, 23 (1932).

10. Hickling, A., and Linacre, J. K., "Glow-discharge Electrolysis. Part II. The Anodic Oxidation of Ferrous Sulphate," J. Chem. Soc., 711 (1954)

11. Manley, T.C., "The Electric Characteristics of the Ozonator Discharge," Trans. Electrochem. Soc. 84, 82 (1943).

12. McAdams, W.H., Heat Transmission, McGraw-Hill Book Co., Inc., New York, N.Y., 3rd Ed., 1954, p.245.

13. Peek, F. W., Jr., Dielectric Phenomena in High-Voltage Engineering, McGraw-Hill Book Co., Inc., New York, N.Y., 1929.

14. Ryan, H. J., "The Conductivity of the Atmosphere at High Voltages," Trans. Am. Inst. Electrical Engineers, 23, 101 (1904).

15. Standard Methods for the Examination of Water and Waste Water, 11th Ed. Amer. Publ. Health Assn., Inc., New York, N.Y. 1960.

16. Staub, F. W., and Brisee, C. G., private communication, Advanced Technology Laboratories, General Electric Company, Schenectady, N. Y.

17. Weiss, J., Allen, A.O., Schwarz, H.A., "Use of the Fricke Ferrous Sulfate Dosimeter for Gamma-Ray Doses in the Range 4 to 40 Kr.," Proceedings of the International Conference on the Peaceful Uses of Atomic Energy, 14, 179, United Nations (1956).

APPENDIX A

APPENDIX A

REACTOR FEED SOLUTION

A solution of ferrous sulfate similar to that used in the Fricke dosimeter[17] was prepared using various concentrations of ferrous ion as needed for the several phases of the experimental program. Sodium chloride and sulfuric acid were used in the quantities specified for the dosimetric solution.

For example, a solution with a concentration of 80 mg Fe^{+2}/l contained:

6 gm $FeSO_4 \cdot 7H_2O$

0.9 gm NaCl

330 ml concn (95-98%) H_2SO_4 in sufficient distilled H_2O to make 15 l.

APPENDIX B

APPENDIX B

ANALYTICAL METHODS

1. Ferric Ion Concentration

A Beckman ratio recording spectrophotometer, Model DK-2, was used to determine the percent of 305 mμ light transmitted by the liquid sample. The instrument was calibrated with a solution of Fe^{+3} of known concentration:

0.386 g $FeCl_3 . 6H_2O$

0.06 g NaCl

22 ml concn. H_2SO_4 were dissolved in 100 ml of distilled water and diluted to 1 liter giving a concentration of 0.080 g Fe^{+3} per liter.

Appropriate dilutions of this master solution were made to determine concentrations of ferric ion which fell within the 20-70% transmission range at 305 mμ with a sample cell having a light path one cm long. The data obtained are shown in Table I and plotted in Figure 1.

2. Nitrate Concentration

The phenoldisulfonic acid method for nitrate in water, as given in Standard Methods[15], was the procedure used in this work.

3. Oxygen Consumed (COD)

The dichromate reflux method for oxygen consumed, as given in Standard Methods[15], was the procedure used in this work.

TABLE I

CALIBRATION DATA - FERRIC CHLORIDE SOLUTIONS

Wavelength = 305 mμ
Temperature = 25°C.

Concentration gm/l	Percent Transmission	Optical Density
0.0040	67.3	.1720
0.0056	55.0	.2596
0.0080	48.8	.3116
0.0096	39.0	.4089
0.0120	31.0	.5086
0.0160	22.8	.6421

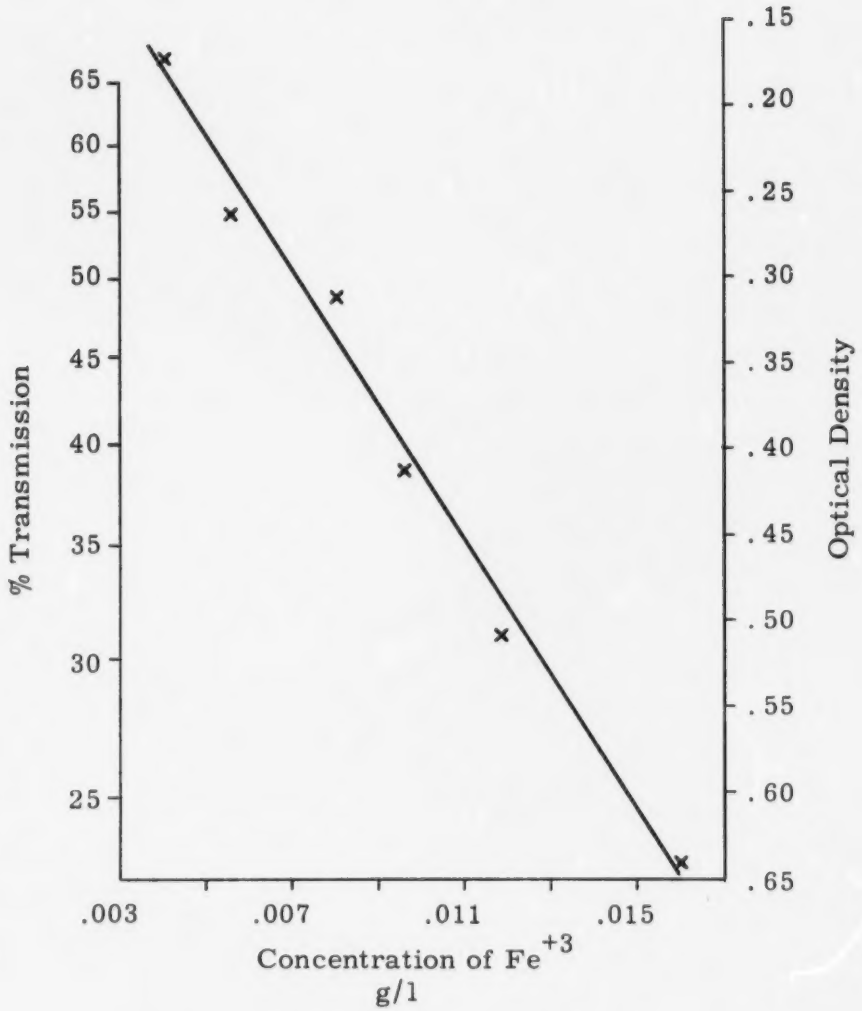

Figure 1. Percent Transmission of Ferric Solutions at 305 mμ (t=25°C).

APPENDIX C

TABLE I

EVALUATION OF CORONA REACTORS: FALLING FILM DATA

Date Aug. 1964	Run No.	Feed Concn. $mgFe^{+2}/l$	Feed Flow Rate l/min.	Gas	Gas Flow Rate $cm^3/min.$	Power, watts	Potential KV Peak	Power Density, $watt/cm^2$	Fe^{+3} Prod. mg/l	Fe^{+2} Conv. %	Yield, $\frac{mgFe^{+3}}{watt\text{-}hr.}$ *	
7	1	80	.50	air	70	308	13.8	.907	27	33.8	2.63	
7	2	80	.50	air	721	308	13.8	.907	32	40.0	3.90	**
7	3	80	.70	air	721	308	13.8	.907	24	30.0	2.34	
10	4	90	.70	air	720	302	14.0	.892	89	99.0	12.4	
10	5	90	.79	air	720	302	14.0	.892	91	100.	14.3	
10	6	90	.68	air	1370	302	14.0	.892	90	100.	12.1	
11	7	90	.50	air	500	60	13.2	.177	27	30.0	13.5	
11	8	90	.50	air	500	135	14.3	.398	41	45.6	9.12	
11	9	90	.50	air	500	265	15.0	.782	57	63.3	6.45	
12	10	82	.50	air	500	220	--	.649	60	73.2	8.18	
12	11	82	.50	air	500	99	13.0	.292	24	29.3	7.27	
12	12	82	.50	air	500	116	--	.342	20	24.4	5.17	
13	13	89	.80	air	500	107	--	.316	15	16.8	6.73	
13	14	89	.26	air	500	105	14.0	.310	46	51.7	6.83	***

NOTES:

* Yield $mgFe^{+3}/watt\text{-}hr. = \frac{1\ feed}{min.} \times \frac{60\ min.}{hr.} \times \frac{mgFe^{+3}\ produced}{1} \times \frac{1}{watts}$

** Poor liquid distribution, larger jet installed after run no. 3.

*** Small jet used for this run.

TABLE II

EVALUATION OF CORONA REACTORS: ROTATING DISK DATA

Date Aug., 1964	Run No.	Elapsed Time, Min.	Feed Conc., $mgFe^{+2}/l$	Feed Flow Rate l/min.	Gas	Gas Flow Rate, $cm^3/min.$	Disk Speed, rev/min.	Power, Watts	Potential, KV	Power Density, $watt/cm^2$	Fe^{+3} Produced, mg/l	Fe^{+2} Conversion, Percent
17	1	35	89	.0080	air	25	4	9.3	9.5	.332	16.5	18.6
18	2a	15	89	.0084	air	25	4	9.6	9.0	.342	18.5	20.8
18	2b	30	89	.0084	air	25	4	9.6	9.0	.342	15.2	17.1
18	2c	45	89	.0084	air	25	4	9.6	9.0	.342	11.8	13.3
18	3a	0	89	.0084	air	25	24	9.6	9.5	.342	12.4	13.9
18	3b	15	89	.0084	air	25	24	9.6	9.5	.342	21.6	24.2
18	3c	30	89	.0084	air	25	24	9.6	9.5	.342	24.6	27.6
18	3d	45	89	.0084	air	25	24	9.6	9.5	.342	18.4	20.7
24	4a	0	89	.0084	air	25	4	---	---	--	0.2	0.2
24	4b	2	89	.0084	air	25	4	11	8.5	.393	8.5	9.6
24	4c	17	89	.0084	air	25	4	11	8.5	.393	20.9	23.5
24	4d	32	89	.0084	air	25	4	11	8.5	.393	15.0	16.8
24	4e	47	89	.0084	air	25	4	11	8.5	.393	25.0	28.1
24	4f	62	89	.0084	air	25	4	11	8.5	.393	31.4	35.2
24	4g	77	89	.0084	air	25	4	11	8.5	.393	24.4	27.4
24	5a	0	89	.0084	air	25	19	---	---	--	0.2	0.2
24	5b	2	89	.0084	air	25	19	9.0	9.0	.321	16.2	18.2
24	5c	17	89	.0084	air	25	19	9.0	9.0	.321	66.5	74.6
24	5d	32	89	.0084	air	25	19	9.0	9.0	.321	61.5	69.1
24	5e	47	89	.0084	air	25	19	9.0	9.0	.321	59.5	66.8
24	5f	62	89	.0084	air	25	19	9.0	9.0	.321	79.5	89.8
24	5g	77	89	.0084	air	25	19	9.0	9.0	.321	76.5	85.9
24	5h	92	89	.0084	air	25	19	9.0	9.0	.321	74.0	83.2
24	5i	107	89	.0084	air	25	19	9.0	9.0	.321	57.0	64.1

TABLE III

SAMPLING VARIABILITY

Feed concentration	88 mg Fe^{+2}/l
Feed flow rate	.285 l/min.
Air flow rate	1.10 l/min.
Power	.87 watts/cm^2
Gap	.30 cm

Sample No.	Sample Size cm^3	Time From Application of Power Min.	Fe^{+3} Concentration mg/l
1	92	10	81
2	160	11	81
3	1950	12	75
4	410	19	81
5	132	20	83

Average 80 $\pm$ 1 mg Fe^{+3}/l

TABLE IV

DETERMINATION OF REACTOR PERFORMANCE CHARACTERISTICS: STAGE I DATA *

Date 1964	Run No.	Feed Concn $mgFe^{+2}/l$	Feed Flow Rate l/min.	Fraction Moisture	Gas Flow Rate $cm^3/min.$	Power, Watts	Potential KV Peak	Power Density, $watts/cm^2$	Fe^{+3} Prod. mg/l	Fe^{+2} Conv. %	Yield, $\frac{mgFe^{+3}}{watt\text{-}hr.}$
10-14	1	80	.525	.42	1180	142	10.5	1.01	70/69	87.5/86.2	15.5/15.3
10-19	2a	41	.360	.22	790	83.2	9.0	.59	40/38/40	97.6/92.6/97.6	10.4/9.9/10.4
11- 2	2b	40	.360	.22	179	80.5	11.6	.58	22.3/22.8	55.7/57.0	5.99/6.12
11- 2	3a	40	.360	.62	1040	78.7/81.6	11.3	.56/.58	18.3/19.3	45.7/48.3	5.04/5.11
11- 4	3b	38	.360	.62	645	80.5	12.0	.58	38/38	100/100	10.0/10.0
10- 7	4a	125	.360	.62	790	205	15.4	1.46	124	99.1	13.1
10- 8	4b	125	.360	.62	790	216	18.0	1.54	108/102	86.4/80.7	11.1/10.5
10- 9	5	128	.360	.22	1530	208	16.8	1.48	120/118	93.8/92.2	12.5/12.3
11- 4	6	38	.690	.62	179	200	--	1.43	38/38	100/100	7.85/7.85
10-20	7	41	.690	.22	1530	211	--	1.51	29/27/41	70.7/65.8/100	5.7/5.3/8.2
10- 9	8a	128	.690	.22	790	77.7	--	.55	6.2/7.4	4.8/5.8	3.2/3.9
10-13	8b	124	.690	.22	790	77.6	10.6	.55	40/38	32.2/30.6	21.3/20.3
11- 5	8c	126	.690	.22	179	65.9/74.0	--	.47/.53	6.2/6.6	4.9/5.2	3.2/3.2
10-13	9a	130	.690	.62	1530	76.3/82.1	9.6/11.4	.54/.59	16.4/34	12.6/26.2	8.9/17.2
11- 5	9b	126	.690	.62	645	83.2	12.0	.59	12/7.2	9.5/5.7	6.0/3.5

NOTE: * Gap .30 cm., Electrode Temperature 25 c. All runs in air.

TABLE V

DETERMINATION OF REACTOR PERFORMANCE CHARACTERISTICS: STAGE II DATA *

Date Nov. 1964	Run No.	Feed Concn. $mgFe^{+2}/l$	Feed Flow Rate, l/min.	Gas Flow Rate cm^3/min.	Power, Watts	Potential KV Peak	Power Density, $watts/cm^2$	Fe^{+3} Produced mg/l	Fe^{+2} Conversion %	Yield $\frac{mgFe^{+3}}{watt\text{-}hr.}$
11	1a	84	.360	790	83.2	14.0	.59	58/62	69.1/73.8	15.1/16.1
11	1b	84	.360	790	83.2	12.0	.59	53/48	63.1/57.1	13.8/12.5
11	2a	84	.360	1530	218/194	15.0/15.5	1.55/1.39	77/79	91.6/94.1	7.6/8.8
11	2b	84	.360	1530	200	15.0	1.43	82/79	97.5/94.0	8.9/8.5
13	3	182	.360	790	200	14.3	1.43	178/174	97.8/95.6	19.2/18.8
13	4	182	.360	1530	79.1	11.5	.57	122/130	67.0/71.5	33.3/35.5
12	5	96	.690	790	200	13.2	1.43	14.6/14.9	15.2/15.5	3.0/3.1
12	6	100	.690	1530	81.0	10.2	.58	29/24	29.0/24.0	14.8/12.3
12	7a	190	.690	790	78.4/88.7	8.4	.56/.63	36/30	19.0/15.8	19.0/14.0
13	7b	178	.690	790	82.4	12.0	.59	34/16	19.1/12.7	17.1/8.04
12	8a	196	.690	1530	208	14.5	1.49	129/126	65.8/64.4	25.7/25.1
13	8b	182	.690	1530	213	11.0	1.52	135/143	74.2/78.6	26.3/27.8

NOTE: * Gap .30 cm., Electrode temperature 70 C. All runs in air. Moisture fraction 0.22

TABLE VI

DETERMINATION OF REACTOR PERFORMANCE CHARACTERISTICS: STAGE III DATA *

Date Nov., 1964	Run No.	Feed Conc., mg Fe^{+2}/l	Feed Flow Rate, l/min.	Gas Flow Rate, cm^3/min.	Power, Watts	Potential, KV Peak	Power Density, watts/cm^2	Fe^{+3} Produced mg/l	Fe^{+2} Conversion, %	Yield mg Fe^{+3}/watt-hr.
23	9	92	.360	790	208	16.0	1.49	90/90	98.8/98.8	9.48/9.48
23	10	92	.360	1530	79.9	13.2	.57	80/82	86.9/89.2	21.6/22.2
27	11a	174	.360	790	79.4	12.5	.57	174/174	100/100	47.4/47.4
30	11b	174	.360	790	76.5	11.5	.55	88/90	50.6/51.6	24.9/25.4
27	12	174	.360	1530	200	17.8	1.43	174/174	100/100	18.8/18.8
24	13	90	.690	790	77.7	11.5	.56	11.3/9.9	12.6/11.0	6.0/5.3
25	14	84	.690	1530	200	--	1.43	22/19	26.2/22.6	4.6/3.9
27	15a	174	.690	790	202	18.0	1.44	33/42	18.9/24.2	6.8/8.6
27	15b	174	.690	790	194	17.0	1.39	174/174	100/100	37.1/37.4
27	16	174	.690	1530	79.9	12.7	.57	9.0/7.4	5.17/4.25	4.8/3.8
Dec.										
** (2	15c	174	.690	790	211	17.5	1.51	152/143	87.3/82.2	29.8/28.1
(2	7c	174	.690	790	79.9	10.5	.57	56/53	31.8/30.4	29.0/27.4

NOTES:

* Gap .30 cm, electrode temperature 70 C. All runs in air, moisture fraction 0.22

** Rerun of No. 15, Stage III and No. 7, Stage II.

TABLE VII

OXYGEN AND ELECTRODE GAP DATA*

Dec., 1964	Run No.	Feed Concn., mgFe^{+2}/l	Gas	Electrode Gap, cm.	Power, Watts	Potential, KV Peak	Power Density, watts/cm^2	Fe^{+3} Produced mg/l	Fe^{+2} Conversion %	mg Fe^{+3}/ watt-hr.
.0	1	168	O_2	.30	79.2	12.0	.57	43/39	25.6/23.2	11.7/10.6
.1	2	174	O_2	.45	58.5	13.8	.42	17.3/20.0	10.0/11.5	6.4/7.4
.0	3	168	Air	.30	78.2	----	.56	92/106	54.8/63.1	25.4/29.3
11	4	174	Air	.45	58.5	14.8	.42	106/65	60.8/37.4	39.2/24.0

NOTES:

* Electrode temperature 75 C. Gas flow rate 1530 cm^3/min.
Feed flow rate 0.360 l/min. Moisture fraction 0.22.

TABLE VIII

MISCELLANEOUS TESTS *

Date	Run No.	Feed Concn., $mgFe^{+2}/l$	Gas	Gas Flow Rate, $cm^3/min.$	Power, Watts	Potential KV Peak	Power Density $watts/cm^2$	Fe^{+3} Produced mg/l	Fe^{+2} Conversion, %	Yield $mgFe^{+3}/watt\text{-}hr.$	Observation
12/29	1	170	Air	790	198	15.0	1.42	156	91.6	32.7	$5.3 mgNO_3/l$
1/4	2	178	Argon	790	77.4	17.0	.55	11/12	6.2/6.7	5.88/6.42	----
1/4	3	332	Air	1530	216	14.5	1.54	224	67.4	42.9	----

* Gap 0.30 cm. Electrode Temperature 70C. Feed flow rate 0.690 l/min. Moisture fraction 0.22

** Nitrate concentration determined by method given in Appendix B

TABLE IX

Reactor Performance with Orga

All runs made with a gas
of 1530 cm^3/l and a feed
of 360 l/min.

Date - December, 1964	15th	15th	15th	15th	15th	15th	16th	16th	16th	16th	16th	16th	17th	17th	17th	17th	17th	17th	18th
Run No.	1-1	1-2	1-3	2-1	2-2	2-3	3-1	3-2	3-3	4-1	4-2	4-3	5-1	5-2	5-3	6-1	6-2	6-3	7-1
Gas	air	air	air	air	air	air	O_2	O_2	O_2	O_2	O_2	O_2	air	air	air	air	air	air	air
Liquid (see Note (1))	A	A	A	B	B	B	C	C	C	D	D	D	E	E	E	F	F	F	G
Power, Watts	80	144	210	80	144	210	80	144	210	80	144	210	80	144	210	80	144	210	80
Power Density watts cm^2	.57	1.03	1.50	.57	1.03	1.50	.57	1.03	1.50	57	1.03	1.50	.57	1.03	1.50	.57	1.03	1.50	.57
Potential, Kilovolts Peak	15.5	13.6	16.5	13.5	13.6	16.5	12.2	13.7	15.8	12.5	13.7	15.8	12.7	14.7	16.3	13.3	14.7	16.3	13.3
Fraction Moisture in Gas	--	--	--	--	--	--	--	--	--	--	--	--	--	--	--	--	--	--	.22
No. of Passes Thru Corona Zone	1	1	1	1	1	1	1	1	1	1	1	1	1	1	1	1	1	1	1
Feed Soln. Treated with O_2	no	no	no	no	no	no	yes	yes	yes	yes	yes	yes	no	no	no	no	no	no	no
Average ΔCOD/l	-9.23	-9.37	-4.17	-3.80	-5.10	-8.20	-1.09	-1.91	-3.08	-2.97	-2.81	-1.94	-3.82	-3.12	-3.08	-.20	-.60	-.60	-1.48
ΔCOD/hr.	-48.16	-49.03	-90.07	-82.08	-110.2	-133.9	-23.54	-41.26	-66.53	-64.15	-47.74	-41.90	-76.03	-67.39	-66.53	-4.32	-12.96	-12.96	-31.97
ΔCOD watt-hr.	-.602	-.341	-.429	-1.03	-.765	-.637	-.294	-.286	-.317	-.802	-.332	-.199	-.950	-.424	-.317	-1.104	-.090	-.0617	-.400
Milliequivalents watt-hr.	.0752	.0426	.0536	.1286	.0956	.0796	.0368	.0358	.0396	.1002	.0415	.0249	.1188	.0585	.0396	.1454	.0112	.0077	.0500
ΔCOD/l after 22 hr. holding period	-.62	-1.47	-1.74	-5.70	-6.10	-6.80	-3.68	-0.30	-3.25	-1.86	-2.69	0.0	-11.77	10.06	-9.02	-5.68	-4.84	-3.84	---
ΔCOD/hr	-13.39	-31.75	-37.58	-79.92	-131.8	-146.9	-79.49	-6.48	-70.20	-40.14	-58.10	0.0	-254.2	-217.3	-194.6	-122.7	-104.5	-82.94	---

NOTES:

(1) Key to Feed Soln.

		Average COD/l
A	Benzoic Acid 10 mg/l	20.4
B	Benzoic Acid 100 mg/l	195
C	Benzoic Acid 16.7 mg/l	33.5
D	ABS Solution 10 mg/l	22.1
E	Secondary Effluent (filtered)	75.6
F	Secondary Effluent cut 1/2 with dist. H_2O	36.4
G	Secondary Effluent (filtered)	72.2
H	Secondary Effluent cut 1/2 with dist. H_2O	36.1
I	ABS Solution 10 mg/l	21.6
J	Carbon Treated Secondary Effluent (filtered)	21.3
K	Secondary Effluent (filtered)	79.8
L	Carbon Treated Secondary Effluent (filtered)	23.3
M	Distilled Water	0.07

(2) Gap .30 cm., electrode temperature 60 C

(3) Run 13-2, feed temperature 40 C

TABLE IX

Reactor Performance with Organic Materials

All runs made with a gas flow rate of 1530 cm^3/l and a feed flow rate of .360 l/min.

17th	17th	17th	18th	18th	18th	18th	18th	18th	21st	21st	21st	21st	21st	21st	22nd	22nd	22nd	22nd	23rd	23rd	23rd	23rd	23rd	23rd	23rd	23rd
6-1	6-2	6-3	7-1	7-2	7-3	8-1	8-2	8-3	9-1	9-2	9-3	10-1	10-2	10-3	11-1	11-2	11-3	11-4	11-5	12-1	12-2	12-3	12-4	12-5	13-1	13-2
air	air	air	air	air	air	air	air	air	air	air	air	air	air	air	air	air	air	air	air	air	air	air	air	air	air	air
F	F	F	G	G	G	H	H	H	I	I	I	J	J	J	K	K	K	K	K	L	L	L	L	L	M	M
80	144	210	80	144	210	80	144	210	80	144	210	80	144	210	144	144	144	144	144	144	144	144	144	144	144	144
.57	1.03	1.50	.57	1.03	1.50	.57	1.03	1.50	.57	1.03	1.50	.57	1.03	1.50	1.03	1.03	1.03	1.03	1.03	1.03	1.03	1.03	1.03	1.03	1.03	1.03
13.3	14.7	16.3	13.3	14.3	15.2	12.7	14.0	16.5	13.6	15.0	16.2	13.6	13.4	16.7	14.3	14.3	14.3	14.3	14.3	14.0	14.0	14.0	14.0	14.0	14.5	14.5
--	--	--	.22	.22	.22	.22	.22	.22	.22	.22	.22	.22	.22	.22	.22	.22	.22	.22	.22	--	--	--	--	--	--	--
1	1	1	1	1	1	1	1	1	1	1	1	1	1	1	2	4	6	8	9	2	4	6	8	10	1	1
no	no	no	no	no	no	no	no	no	no	no	no	no	no	no	no	no	no	no	no	no	no	no	no	no	no	no
+.20	-.60	-.60	-1.48	-3.64	-5.22	-5.06	-4.86	-4.62	+1.40	+1.12	+3.05	-1.40	- 84	-.70	-2.74	-8.55	-6.98	-5.02	-5.69	-1.50	-.01	+3.53	-12.79	+11.54	-1.76	+5.15
-4.32	-12.96	-12.96	-31.97	-78.62	-112.8	-109.3	-105.0	-99.79	+30.24	+24.19	+65.88	-30.24	-18.14	-15.12	-59.18	-184.7	-150.8	-108.4	-122.9	-32.40	- 216	+76.25	+278.3	+249.3	-38.0	+111.2
1.166	-.090	-.0617	-.400	-.546	-.537	-1.366	-.729	-.475	+.375	- 168	+.315	-.378	-.126	-.072	- 411	-1.282	-1.047	-.753	- 854	-.225	-.0015	+.530	+1.918	+1.731	- 394	+.772
.1458	.0112	.0077	.0500	.0682	.0671	.1708	.0911	.0594	.0472	.0210	.0392	.0448	.0158	.0090	.0514	.1600	.131	.0941	.1068	.0281	.0002	.0662	.2396	.2164	.0330	.0966
-5.68	-4.84	-3.84	---	---	---	---	---	---	---	---	---	---	---	---	---	---	---	---	---	---	---	---	---	---	---	---
122.7	-104.5	-82.94	---	---	---	---	---	---	---	---	---	---	---	---	---	---	---	---	---	---	---	---	---	---	---	---